STUDY ON SOLAR HYDROGEN GENERATION FROM WATER

Thesis submitted by

Suman Das

Master of Chemical Engineering

Class Roll no: **002010302007**

Exam Roll no: **M4CHE22007**

Registration Number: **131173 of 2015-2016**

Under the guidance of

Dr. (Prof) Kajari Kargupta

Professor

Chemical Engineering Department

Jadavpur university

Kolkata, India-700032

2022

Acknowledgment

I would like to express my gratitude for the help, cooperation, and inspiration that I have received from my teachers, friends, and well-wishers during this course. It is their kind help and untiring effort that has resulted in the completion of this project.
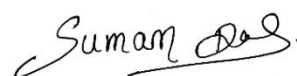
I am highly obliged and grateful to my Project Coordinator **Prof. Kajari Kargupta**, for her excellent guidance, endless encouragement, and cooperation extended to me from the onset of this task until its successful completion.

I am very grateful to **Prof. Rajat Chakraborty**, Head of the Chemical Engineering Department, for all the necessary help I got during my project work.

I am also indebted to **Jadavpur University, Dept. of Chemical Engineering,** for supporting me and giving me the opportunity to use the equipment to do my research.

My sincere appreciation also extends to all my lab mates, **Miss Arundhati Sarkar**, **Mr. Sayantanu Mandal,** and **Mr. Arindam Mandal** who have provided assistance on various occasions. I would also like to extend my thanks to our Lab assistant **Mr. Ajay Kumar Prodhan,** who has helped me a lot throughout my work.

I am grateful to my parents and all of my family members who encouraged and supported me all through and helped me in all respect.

Suman Das.

_____

Suman Das

****

CERTIFICATE

This is to certify that **Mr. Suman Das**, Final year Masters of Chemical Engineering (M.ChE) examination student of Department of Chemical Engineering, Jadavpur University, Class Roll No**. 002010302007**, Registration No. **131173 of 2015- 2016**, Examination Roll No. **M4CHE22007** has completed the Project work titled, **"Study on Solar Hydrogen Generation from Water"** under the guidance of **Prof. Kajari Kargupta** during his Master's Curriculum. This work has not been reported earlier anywhere and can be approved for submission in partial fulfilment of the course work.

_____   _____

Prof. Rajat Chakraborty   **Prof. Kajari Kargupta**

Head of the Department and Professor   Project Supervisor, Professor

Chemical Engineering Department   Chemical Engineering Department

Jadavpur University   Jadavpur University

_____

Signature of the Dean

TABLE OF CONTENTS

****

TABLE OF FIGURES

LIST OF TABLES

Abstract

Water splitting for hydrogen production under solar light irradiation is an ideal system to provide renewable energy sources and to reduce global warming effects. Even though significant efforts have been devoted to fabricate advanced nanocomposite photo-catalysts, the main challenges persist, are slow reaction, lower rate of H_2 evolution, high recombination rate of photogenerated electrons and holes, metal loss of powder form of photocatalyst and lower retention of reacting species on these photocatalyst that limits the feasibility of continuous mode of operation.

These issues are addressed introducing alginate-based hydrogel having higher water adsorption and retention capacity to encapsulate different photocatalysts namely CdS, rGO-CdS and to form beads like Photocatalysts. The powder form of CdS and rGO-CdS as well as the beads form of alginate encapsulated photocatalysts (CdS-alginate, rGO-CdS-alginate) are successfully synthesised, characterized and tested for photocatalytic hydrogen generation under full band solar irradiation using a solar simulator. Among all the synthesised catalysts, **CdS-rGO-alginate** exhibits the maximum photocatalytic activity of **79.6** mmol/g. hr which is more than that of **CdS -alginate** (**55.62** mmol/g.hr) and remarkably higher than that of pristine CdS powder catalyst (**4.88** mmol/g.hr). Band pass filter of 420 nm is used in the system to evaluate the apparent quantum yield (AQY) of the process. Among all the synthesized catalysts, **rGO-CdS -alginate** exhibits the maximum AQY of **18.24%** at **420** nm of band pass filter. It may be inferred that use of alginate having plenty of OH- groups promotes the water adsorption into its confined porous structure and causes the chemisorption of water molecules on the surface of photocatalyst (CdS/ rGO-CdS).

****

Chapter-1

Introduction

Introduction

Natural resources such as coal and petroleum products as a source of energy are nearly exhausted[1]. Reducing fossil fuel reserves has prompted substantial research efforts toward using Hydrogen (H_2) as an environmentally friendly energy carrier for the post-fossil fuel regime [1].

Humans have been utilizing fossil resources for energy and development since the Industrial Age began with the creation of the steam engine in the 1760s. However, the predicted depletion of fossil fuel reserves after more than 150 years of exploitation and use has highlighted energy sustainability. To reduce our reliance on fossil fuels, it is critical to create renewable energy sources. Solar energy is the most exploitable renewable energy resource that might supply present and future human energy demand. Only 0.015 % of solar energy hitting the planet is predicted to be sufficient to support human society.

Hydrogen is an up-and-coming candidate as a future energy carrier. It is attractive to produce Hydrogen from solar energy and seawater, the most abundant renewable energy source and the most abundant natural resource on the earth[2]. H_2 may be the best solution for addressing the triple challenges of exhaustion, pollution, and climate change effects, according to the current consensus.

1.1 Hydrogen as a future fuel

Hydrogen is considered an energy carrier, not a primary energy source. It is considered as the dream fuel of the future. The only material that can be produced from the burning of Hydrogen in air is water, a renewable, eco-friendly product. Therefore, no pollutant is released that might have a negative effect on global warming, the ozone layer, and climate change.

Hydrogen is a promising option for replacing fossil fuels. Table 1.1 displays the physical and chemical properties of Hydrogen compared to those of some of the fossil fuels. The energy of each fuel can be represented by the value of heat produced from the complete combustion of that fuel.

Fuel	Density (g/l)	Lower heating Value (MJ/kg)	Carbon Percentage %
Crude oil	845	42.8	85.0
Natural gas	0.654	50.1	75.0
Conventional Gasoline	737	43.7	85.5
Conventional Diesel	856	41.8	87.0
Hydrogen	0.0818	121.0	0

Table 1.1: The energy content of different fuels

Despite the abundance of a large amount of Hydrogen in the universe, nearly all of it exists as a compound, rather than in its pure form. Thus, to use it as fuel, it has to be extracted from its compounds by several methods, as shown in the next section.

The economy of the world depends on what type of energy source is used, and eras are named according to those sources. Two hundred and fifty years ago, the invention of the steam engine gave the name to that era of modern technology. However, due to the extraction of fossil fuels and their use in all aspects of daily life, the world moved into the petroleum epoch. The considerable amount of research regarding the development of the production and application of hydrogen fuel has prepared the world to receive a new era, that is, the era of Hydrogen.

The hydrogen economy, or the hydrogen market, is a term introduced by John Bockris during his talk in 1970 at General Motors (GM) Technical Centre; it covers the generation of Hydrogen from renewable and non-renewable energy sources, the storage, transportation, and the application. There is controversy about the feasibility of a hydrogen economy. The components of this technology claim that the use of hydrogen fuel has many advantages in terms of economic and energetic considerations:

- It is an environmentally friendly fuel; water is the only by-product of the combustion of Hydrogen and there are no greenhouse gases.
- Decentralization of energy generation: because of the inherent nature of some areas for fossil fuels, the economy of developed and developing countries depends on oil importation. Additionally, some of them have reached their oil peak. In contrast, the production of Hydrogen will not be limited to those countries, as Hydrogen can be produced anywhere as long as water and electricity are available.
- Because of the abundance of Hydrogen and because it can be produced from many cheap renewable energy sources, as mentioned previously, it will be considered the 'forever fuel'. On the other hand, a hydrogen economy faces several obstacles, which are still the subject of controversy among scientists.
- Currently, 48% of the global supply of Hydrogen is produced from natural gas, 30% from oil, 18% from coal and only 4% from electricity. Hydrogen production from fossil fuels creates CO_2, that is, greenhouse gases. Furthermore, nitrogen oxides can be formed on account of hydrogen leakage. Consequently, developing technologies that can overcome CO_2 emission and the use of fossil fuels is a major target.
- Currently, the cost of generating and transporting Hydrogen is greater than the cost of extracting, processing and transporting gasoline.

- Storage is one of the most important aspects of a hydrogen economy. Hydrogen can be stored as a compressed gas, as a liquid or by dissolving hydrogen gas in a metal. In addition, it can be stored as a solid in different types of chemicals, such as carbon nanotubes, or amine borane complex. The difficulties of hydrogen storage methods are almost all concerned with the storage density, which in turn affects its transportation. "The physical limits for the storage density of compressed and liquid Hydrogen have more or less been reached, while there is still potential in the development of solid materials for hydrogen storage, such as systems involving metal hydrides. So, the issues arising from the storage and transportation technologies of Hydrogen can be overcome by continual research to make these technologies more convenient and economical.
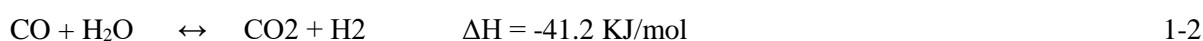
1.2 Different methods of Hydrogen production

There are different methods to produce H_2 using solar energy. The most common process of converting solar energy into electricity is through photovoltaic cells. However, the electricity is difficult to store and distribute over long distances, or it must be used immediately. Electrolysis/photolysis of water, biological hydrogen production, natural gas reforming, coal gasification, and methanol/ethanol pyrolysis are now the most common hydrogen production processes[2]. Table 1 compares the advantages and disadvantages of several hydrogen-generating approaches.

All current hydrogen generation technologies, such as natural gas reforming, coal gasification, and methanol/ethanol pyrolysis, consume a lot of electricity and pose a severe threat to the environment and modern society's long-term viability [3]. Although the electrolysis of water is a highly effective method, it consumes a lot of electricity. The methods of biological Hydrogen production are still in their infancy. The main challenge right now is how to manufacture vast amounts of hydrogen energy in a cost-effective, environmentally friendly, and long-term manner.

a. Steam reforming

Steam Methane Reforming (SMR) was developed in 1930 and became one of the most important processes for hydrogen production. The Principle reaction of SMR is presented by the following equations:

$$CH_4 + H_2O \quad \leftrightarrow \quad 3H_2 + CO \qquad \Delta H = 206.2 \ KJ/mol \qquad\qquad 1\text{-}1$$

$$CO + H_2O \quad \leftrightarrow \quad CO2 + H2 \qquad \Delta H = \text{-}41.2 \ KJ/mol \qquad\qquad 1\text{-}2$$

$$CH_4 + 2H_2O \leftrightarrow 4H_2 + CO_2 \qquad \Delta H = 165 \text{ KJ/mol} \qquad \text{1-3}$$
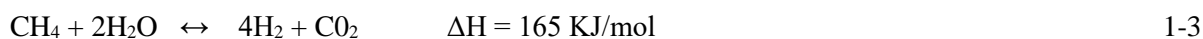
This process is reversible and endothermic, so it is carried out at 700 -900 °C and 15 - 30 * 10^5 Pa with nickel supported on alumina as a catalyst. Despite the importance of this method, it faces some problems and limitations:

- hydrogen production is limited to the equilibrium conversion of methane owing to the reversibility of the reaction.
- it has CO_2 production as a by-product, which affects climate change.
- there is catalyst deactivation due to carbon formation; therefore, there is a limit to the lifetime of the catalyst, and finally
- this process relies on the use of a fossil fuel (methane).

b. Electrolysis

Another method to produce Hydrogen is the splitting of water into H_2 and O_2 when an electric current is sent through the water. This process is called electrolysis; it consists of an oxidation process at the anode to produce oxygen, and a reduction process at the cathode to produce Hydrogen, as observed in the following equations:

Cathode (Reduction):

$$2H_2O \text{ (I)} + 2e^- \rightarrow H_2 \text{ (g)} + 20H^-\text{(aq)} \qquad \text{1-4}$$

Anode (Oxidation):

$$4OH \text{ (aq)} \rightarrow O_2 \text{ (g)} + 2H_2O \text{ (I)} + 4e^- \qquad \text{1-5}$$

Overall:

$$2H_2O \rightarrow 2H_2 \text{ (g)} + O_2 \text{ (g)} \qquad \text{1-6}$$

This process is slow if the above reaction occurs in pure water, so an electrolyte (such as potassium chloride) must be added.

Hydrogen produced by electrolysis accounts for about 4% of production worldwide. Most of it is produced as a by-product of chlorine production. The efficiency of the electrolysis of water is about 50-80% to convert the electrical energy to Hydrogen's chemical energy.

c. Thermochemical production

Splitting water into Hydrogen and oxygen in this case can be achieved by using high temperature heat, though not electricity as in electrolysis, since thermal energy is cheaper than electrical energy. This method has great potential in the hydrogen economy. The heat source can be from concentrated solar energy that generates high temperatures reaching 2,000 °C. In addition, nuclear power supplies heat that reaches 1,000 °C.

d. Reforming of biomass and waste

Hydrogen can be produced from biomass and wastes as new renewable energy sources. The gasification of biomass is efficient, environmentally friendly, and has operational advantages. This process is classified according to the type of gasifying agent: air, steam, steam oxygen, air-steam, oxygen-enriched air, and so on [12, 13]. There have been extensive studies regarding hydrogen production from waste materials and wastewater from industrial processes. The problems arising from this method are the low hydrogen production rate and yield.

e. Photolysis

Two decades ago, great interest was shown in the photochemical reduction of water to generate Hydrogen. Photolysis of water, photodecomposition, involves splitting water into Hydrogen and oxygen using the photons. In other words, it is the conversion of photon energy to chemical energy, which is stored as hydrogen fuel. This process is presented in equation 1-7:

$$H_2O \ (l) + hv \qquad \rightarrow \qquad H_2 \ (g) + \tfrac{1}{2} \ O_2 \ (g) \qquad\qquad 1\text{-}7$$
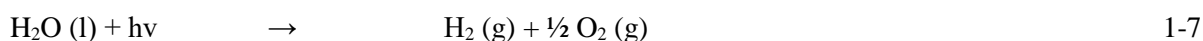
Photocatalytic water splitting

1. Photocatalysis

A catalyst increases the rate of chemical reactions by reducing of the activation energy; therefore, many people have been searching for a catalyst to increase the rate of water splitting. "Photocatalysis is the acceleration of a photoreaction by the presence of a catalyst". Heterogeneous photocatalysis involves two kinds of photoreaction. On the one hand, if the catalyst interacts with a photo excited adsorbed molecule, the process is called a catalysed photoreaction. On the other hand, if the adsorbate molecule interacts with the photo excited catalyst, the process is referred to as a sensitized photoreaction.

After the innovative work by Fujishima and Honda, which involved the photo-electrocatalytic water splitting on TiO_2 electrodes, there have been a significant number of studies in the field of heterogeneous photocatalysis.

Fujishima and Honda's work is a simulation of what occurs in nature, since during the photosynthesis process that takes place in plants, CO_2 and water, readily available materials, are converted to O_2 and carbohydrates using solar energy. Therefore, photosynthesis has been taken as a model for artificial photosynthesis in the generation of Hydrogen as a clean fuel from solar energy.

The significance of photocatalysis stems from the possibility that it can achieve an enormous number of reactions, which can play a significant role in economical and commercial development. Because of the promising features of the photocatalytic processes, they are applied in the following technologies as a replacement for traditional methods:

a) Synthesis of organic compounds: Some reactions, such as oxidation and oxidative cleavage, reduction, isomerization, substitution, and polymerization, can be accomplished using TiO_2 in an oxidatively inert solvent.

b) Synthesis of inorganic compounds: Photocatalysis has attained significant importance in the synthesis of coordinatively unsaturated species, transition metal compounds with a changed oxidation state, free ligands and ligand redox products.

c) Air purification: Air pollution is among the threats to humans and other living organisms, as it causes climate change, global warming, and ozone depletion. This problem has grown in recent years owing to the industrial revolution and the population explosion. Because of the limitations of the conventional methods used in air cleaning, photocatalytic detoxification technology is of great interest.

d) Water purification: The developed and developing countries in particular face a major environmental problem, that is, water pollution, even though it is considered a global issue. Photocatalytic degradation is an alternative method in the treatment of wastewater. This technology has proved its success and effectiveness for the removal of persistent organic and inorganic impurities.

e) Solar energy conversion: Solar energy is versatile since it can be converted to electricity, heat and fuel. Hydrogen as fuel can be generated from sunlight and water, both are renewable sources. This method, which is known as solar water splitting, has gained great importance due to it providing clean, renewable fuel.

in recent years, studies have focused on developing methods to obtain the maximum efficiency of solar conversion and quantum yield, and, therefore, to meet the energy requirements of large-scale

manufacturing and practical uses. Several methods have been used to generate hydrogen fuel from solar water splitting; these have varying restrictions, such as direct or indirect photo thermal, photosynthetic, photo electrochemical limitations. Below table summarises the limitations and potential of these processes.

Process	Limitations, potential
Photosynthetic, biological & photochemical	Demonstrated efficiencies very low, Generally< 1 % solar energy conversion
Photo thermal, single step(direct)	Gas recombination limitations, high temperature material limitations, generally < 1 % solar energy conversion
Photo thermal, multistep	Lower temp than single step, although stepwise reaction inefficiencies lead to losses, generally < 10% solar conversion
Photo electrochemical	10-20% solar conversion
photo thermal, electrochemical	potential for > 20% solar conversion, requires solar concentration

Table 1.2 Potential and limitation of different photocatalysis process

2. Fundamental mechanism of semiconductor photocatalysis

When sufficient light energy is absorbed by a semiconductor material, an electron is promoted from the highest level of the valence band (VB) to the lowest energy level in the conduction band (CB), as depicted in Fig. 1.1. This light must be at a wavelength less than or equal to the equivalent band gap energy (E_g), which is assumed to be constant in the bulk material. The photogenerated electron–hole pair has a number of competing possible pathways and these can be controlled through surface modifications and addition of electrolytes or reactive redox species. These excitation pathways are bulk recombination via inter-bandgap states, light emission through direct excited recombination, recombination via crystal surface states, electrons lost in the CB to an electrochemical process, and holes lost in the valence band to an electrochemical process. For ideal H_2S and H_2O splitting, the latter two processes should be dominant in redox reactions for O_2, S and H_2 formation. Anodic oxidation

processes are critical in the dissolution of the surface of nanoparticles. For sulfides, dissolution yields sulphite and sulphate species and the associated metal counter ion in solution. When a particle moves from the 3D bulk structure to a dimensionless nanoparticle with a radius less than that of the Bohr radius, quantum confinement occurs. This has a significant effect on the energetics and physics of semiconducting materials. As the radius of a nanoparticle decreases below the Bohr radius, which is approximately 5 nm for most semiconductors, the bandgap increases, decreasing the absorption and emission wavelengths of the semiconductor. This can be an issue in obtaining visible-light excitation. The redox properties of a photo excited semiconductor depend predominantly on the energetic positions of the highest energy state of the valence band and the lowest energy state of the Conduction band. It is evident from reactions that the quasi-Fermi level of electrons in the Conduction band must be 4.0 eV to catalyse reduction of water to Hydrogen, and similarly the quasi-Fermi level of holes in the valence band must be 1.23 eV to oxidize water in the relatively unfavourable four-hole process:
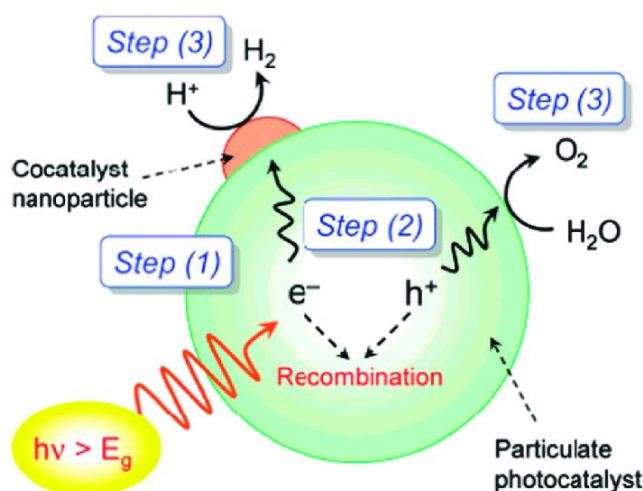
$$2H^+ + 2e^- \rightarrow H_2 \ (E^0_{Red} = 0 \ eV) \hspace{4cm} 1\text{-}7$$

$$2H_2O + 4h^+ \rightarrow O_2 + 4H^+ \ (E^0_{Ox} = -1.23 \ eV) \hspace{3cm} 1\text{-}8$$

Fig. 1.1 Mechanism of photocatalytic hydrogen production from water

3. Principles of photocatalytic hydrogen generation

In Fujishima and Honda's pioneering work, the electrochemical cell they constructed for the decomposition of water into Hydrogen and oxygen is shown in Figure 1.1. When the surface of the photocatalyst was irradiated by UV light, as a result of a water oxidation reaction, oxygen evolution occurred at the TiO_2 electrode. Concomitant reduction led to hydrogen evolution at the platinum black

electrode. This concept, which emerged from the use of photo electrochemical cells with semiconductor electrodes, was later applied by Bard to the design of a photocatalytic system using semiconductor particles or powders as photocatalysts.

A photocatalyst absorbs UV and/or visible (Vis) light irradiation from sunlight or an illuminated light source. While the holes are kept in the valence band of the photocatalyst, the electrons are stimulated to the conduction band. The result is the formation of the pairs of negative electrons (e^-) and positive holes (h^+). The energy difference between the valence band and the conduction band is referred to as the "band gap" in this stage, which is also known as the "photo-excited" state of the semiconductor. In order for the light to be successfully absorbed by the photocatalyst, this must match the wavelength of the light. Following photoexcitation, the energised electrons and holes split and go to the photocatalysts surface. Here, they function as reducing and oxidising agents, producing H_2 and O_2, respectively, in the photocatalytic water-splitting Mechanism. Figure 1.1 shows a schematic illustration of the photocatalytic system for operating Principle.

Water splitting into H_2 and O_2 is an uphill reaction. It needs the standard Gibbs free energy change ΔG^0 of 237 kJ/mol or 1.23 eV, as shown in equation 1-9.

$$H_2O \quad \rightarrow \quad \frac{1}{2} O_2 + H_2; \Delta G = +237 \text{ kJ/mol} \qquad\qquad 1\text{-}9$$

Therefore, the band gap energy (E_g) of the photocatalyst should be >1.23 eV (400 nm).

The matching of the band gap and the potentials of the conduction and valence bands is crucial to enable both the reduction and oxidation of H2O by photo excited electrons and holes. Both the reduction and oxidation potentials of water should lie within the band gap of the photocatalyst. The top level of the valence band must be more positive than the oxidation potential of O_2/H_2O, while the bottom level of the conduction band must be more negative than the reduction potential of H^+/H_2 (0 V vs. normal hydrogen electrode (NHE)) (1.23 V).

We can see that there are many semiconductor systems whose electronic structures match well with the redox potential of water into Hydrogen and oxygen molecules. The band structure requirement is a thermodynamic requirement for water splitting. Other factors, such as over potentials, charge separation, mobility, and lifetime of photogenerated electrons and holes, affect the photocatalytic generation of Hydrogen from water splitting as well. For example, the band edges of the semiconductor photocatalyst usually vary with the change of pH, The phase stability of the semiconductor photocatalyst changes in different pH environments as well.

4. Main Processes of Photocatalytic Hydrogen Generation

The semiconductor photocatalyst must first have a low band gap to absorb as much light as possible, followed by the generation of excited charges (electrons and holes), recombination of the excited charges, separation of the excited charges, migration of the excited charges, trap of the excited charges, and transfer of the excited charges and reflection or scattering of light by the photocatalyst should be minimized. Second, using the absorbed photons, the semiconductor photocatalyst should have a high efficiency in generating excited charges, instead of generating phonons or heat.

After excited charges are created, charge recombination and separation/migration processes are two important competitive processes inside the semiconductor photocatalyst that largely affect the efficiency of the photocatalytic reaction for water splitting. Charge recombination reduces the excited charges by emitting light or generating phonons. It includes both surface and bulk recombination and is classified as a deactivation process, and it is ineffective for water splitting. The separation of excited electrons and holes sometimes may need to overcome an energy barrier, which is the binding energy of the excited electron-hole pairs, and excitons. Charge separation and migration, on the other hand, is an activation process. This is as a result of the charges being on the surface of the photocatalyst ready for the desired chemical reaction. It is beneficial for hydrogen generation through water splitting. Efficient charge separation and fast charge transport, avoiding any bulk/surface charge recombination avoided, are fundamentally important for photocatalytic hydrogen generation through water splitting. Any approach beneficial to the charge separation and transport should be taken into account such as design of internal-built electric field and use of high photoconductive semiconductor materials.

The reaction of photogenerated H_2 and O_2 to form H_2O on the photocatalyst surface is normally called "surface back reaction (SBR)". It will inevitably have a negative effect on any enhancement of the photocatalytic activity, because it reduces the amount of H_2 emitted from the photocatalyst. There are two main approaches to suppress SBR: one involves the addition of sacrificial reagents into the photocatalytic reaction environment and the second creates a separation of the photoactive sites on the surface of the photocatalysts. In general, the electron donor and acceptor sacrificial reagents that are added work as an external driving force for the surface chemical reaction and depress the H_2O formation from H_2 and O_2. The separation of the photoactive sites necessary for hydrogen and oxygen evolution, and which is always accompanied by the surface separation of the photogenerated electrons and holes, has been shown to be greatly affected by the surface properties of the photocatalysts. As well as the surface reaction sites themselves, the surface states and morphology also play an important role.

Chapter - II

Literature review

Aims & Objectives

Literature Review

This chapter introduces some information about the literature surveyed and reviewed to execute present investigation. Several studies involving graphene and graphene based nano particles for hydrogen generation are performed all over the world for the last few years. In this part of study an effort has been made to identify some of the main facts, which may have some impact on performance and morphological characterization of the catalysts and their effect on hydrogen generation. Few of these are given below:

Title of the paper	Journal name	Authors	Year of publication	Volume	Page Number	Description
A critical review in strategies to improve photocatalytic water splitting towards hydrogen generation [38]	International journal of hydrogen energy	Nur Farjina, Muhammad Tahir	2019	44	540-577	Recent developments in photocatalysts, fabrication of novel heterojunction constructions and factors influencing the photocatalytic process for dynamic hydrogen production have been discussed. Development in TiO_2 and g-C_3N_4 based photocatalysts and their potential for H_2 production

						are extensively studied.
Photocatalytic water splitting utilizing electro span semiconductor for hydrogen generation, fabrication, modification and performance. [37]	BCSJ	Xiao ling Lang, Saianand Gopalan, Wanlin Fu and Seeram Ramakrishna	2020	94	8-20	Significant advancements in the creation of adaptable electrospinning-based semiconductor photocatalysts for water splitting. Structure and compositional modifications and performance-improving techniques for a variety of metal electro spun semiconductors are examined.
Solar hydrogen generation from seawater with a modified BIVO$_4$ photoanode. [31]	Energy Environ Sci	Wenjun Luo, Zaisan Yang, Zhaosheng Li, Jiyuan Zhang, Jianguo	2011	4	4046-4051	After modification, a multi-metal oxide BIVO$_4$ is used as the foundation for an

		Liu, Zongyan Zhao, Zhiqiang Wang, Shicheng Yan, Tao Yu and Zhigang Zou				effective and reliable method for seawater splitting. The results showed that modified BIVO4 had the highest IPCE at 1.0 VRHE in the visible light region of 440–480 nm among all known oxide photo anodes, with a photocurrent density of 2.16 mA /cm^2 at 1.0 VRHE in natural seawater under AM 1.5G sunshine (1000 W /m^2).
Graphene Based Materials for Hydrogen Generation from Light Driven	Advanced Materials	GuancaiXie , Kai Zhang, Beidou Guo, Qian Liu, Liang	2013	25	3820-3839	A brief introduction of the basic principles of hydrogen generation

Water Splitting [32]		Fang, and Jian Ru Gong				from solar water splitting, and tailoring properties of graphene are discussed in this paper. Then, the roles of graphene in hydrogen generation reaction, including an electron acceptor and transporter, a cocatalyst, a photocatalyst, and a photosensitizer, are elaborated respectively.
Semiconductor-based Photocatalytic Hydrogen Generation. [33]	Chem. Rev.	Xiaobo Chen, Shaohua Shen, Liejin Guo, and Samuel S. Mao	2010	110	6503-6570	The sacrificial reagent-containing water-splitting systems constructed based on the Pt/CdS, Pt-PdS/CdS and

						Zn/Cr layered double hydroxide photocatalyst demonstrated the best performance for hydrogen production and oxygen production, with the highest quantum yields of ca. 60.35%, 93%, and 60.1%, respectively, at 420 nm.
Nano-casting procedure for catalytic cobalt oxide bead preparation from calcium-alginate capsules: Activity in ammonia borane hydrolysis reaction. [34]	Applied Materials Today	Beyza Nur Kinsiz , Bilge Cos¸kunerFiliz , Serpil KılıçDeprenc , AyselKantürkFigen	2021	22		In the paper, the nano-casting procedure was adapted to cobalt oxide (Co_3O_4) micro beads preparation by multi-step ions exchange procedures. By nano-

						castings -, cobalt-alginate capsules provided the formation of a surface-active bead $(140 \pm 0.4$ μm) in Co_3O_4 nanoparticles (25–35 nm) with enhanced performance for releasing of Hydrogen from NH_3BH_3. Moreover, the catalysts used for 555 min without any mechanical damages during reusability tests and regeneration procedure.
Heterogeneous photocatalyst materials for water splitting. [35]	Chem Soc Rev	Akihiko Kudo and Yugo Misekl	2009	38	253-278	This paper shows the basis of photo catalytic

						water splitting and experimental points, and surveys heterogeneous photocatalyst materials for water splitting into H_2 and 0_2, and H_2 or 0_2 evolution from an aqueous solution containing a sacrificial reagent.
A review on the development of visible light responsive WO_3-based photocatalysts for environmental applications. [36]	Chemical engineering journal advances	J.C. Murillo-Sierra, A. Hernández Ramírez, L. Hinojosa-Reyes, J.L. Guzmán-Mar	2021	5		Based on their use in environmental applications like the elimination of organic pollutants, air purification, CO_2 photo reduction, hydrogen production from water splitting, and most

						recently, the simultaneous production of electricity and wastewater treatment by photo catalytic fuel cells, the photo catalytic properties of the WO_3 based photocatalysts are discussed.
A visible light-driven photocatalysis process by alginate beads coupled with in-situ cadmium sulfide prepared for decontamination in aqueous solutions with treatment of chromium as an example. [39]	Chemical engineering journal advances	Kok Yuen Koh, Zhihao Chen, Zhongrong Du, Sikal Benjamin Ngeow, J.Paul Chen	2022	11		An innovative photocatalysis process with alginate beads coupled with cadmium sulfide was developed for decontamination in waters via visible light. This study provides a stable CdS-SA bead for

						an effective and efficient photocatalytic reduction of Cr(VI) in the water under the visible light.

Table 2.1 Literature Review

2.1 Summary of literature review

After the extensive literature review it is observed that there are so many advantages and some of the research gap of this process. Process bottle necks and advantages of the process are discussed below.

Process Bottlenecks

- Rapid recombination of photo generated electrons and holes
- Low yield hydrogen production
- Slow kinetics due to low retention time of water molecule on active sites
- The usual operational mode of photocatalytic hydrogen generation is in batch mode: Limitation in industrial application

2.2 Role of adsorbent on photocatalytic water splitting

Slow kinetics is one of the major process bottlenecks for hydrogen generation by water splitting from both liquid and vapour phases. On the other hand, thermodynamically backward reaction (formation reaction of water) is more favourable than the forward reaction (splitting reaction). As photocatalytic water splitting reaction involves adsorption and heterogeneous surface catalysed reaction, there are two controlling resistances:

i) Adsorption controlling

ii) Reaction controlling

Water splitting reaction follows slow kinetics so water molecule does not get sufficient retention time for the reaction with photocatalyst. So, high retention time is very much needed for water splitting reaction so adsorption step is a crucial step for water splitting reaction. Novelty of our work is to

incorporation of adsorbent into photocatalyst. Adsorbent has main two roles in photocatalytic water splitting.

i) **Adsorption of water molecule**

ii) **Provides high retention time for the reaction:** Adsorbent is polymeric material containing –OH, -NH$_2$, -COOH group so that water molecule can get attached by inter molecular hydrogen bonding. Various polymeric adsorbents are tested and selection is done based on the adsorption capacity.

Choice of Sodium-Alginate

Sodium alginate is a biopolymer containing –OH and –COOH with six membered cyclic ring. It has a very good moisture adsorbing capacity due to the presence of these functional groups. Water molecule is held by intermolecular hydrogen bonding with hydroxyl and acid groups. As pristine CdS is insoluble in water, so retention time of water molecule on active sites of CdS is very less. As sodium alginate is moisture adsorbing polymer, so it adsorbs water molecules on active sites of photocatalyst when composite is formed and provides sufficient time for reaction. Thermodynamically, water splitting reaction is not preferable (ΔG^0 =237.18 KJ/mole) so large retention time is the key factor for water splitting reaction to produce Hydrogen.
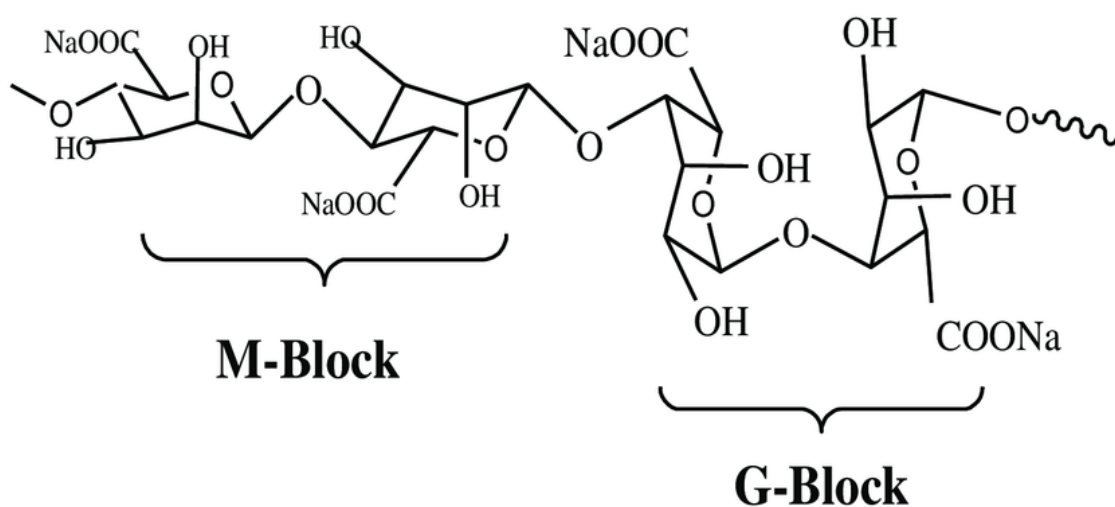

Fig. 2.1 Molecular structure of Sodium Alginate

2.3 Tailoring Properties of Graphene for Photocatalytic H$_2$ Generation

Pure carbon atoms are organised in a regular hexagonal arrangement to form the substance known as graphene. One atom thick layers of graphite are what are known as graphene. Due to its outstanding qualities, including high optical transmittance, strong electrical conductivity, high flexibility and a

higher theoretical surface area, and exceptional chemical stability, it has received a lot of attention. Therefore, graphene can be used for:

a. Graphene as an Electron Acceptor and Transporter

Due to its high work function (4.42 eV), [17] graphene can accept photogenerated electrons from the CBs of most semiconductors or the lowest unoccupied molecular orbitals (LUMO) of dyes with no barrier, which will efficiently suppress the recombination of photogenerated charges and significantly enhance their photocatalytic H_2 -production activity. Furthermore, graphene possesses exceptionally high conductivity, so the accepted electrons can migrate rapidly across its 2D plane to reactive sites for H_2 evolution. Therefore, the role of graphene as an electron acceptor and a transporter has been extensively investigated to enhance the PEC/photocatalytic H_2 -production activity recently, and many encouraging findings are already obtained in both UV- and visible light-active systems.

b. Graphene-Based UV-Active System

A variety of wide bandgap semiconductors have been combined with graphene for photocatalytic reactions under UV-light irradiation, such as TiO_2, [10] ZnO, [12] ZnS, [15] 6H-SiC, [12] and BiOCl. [17] Among them, only TiO_2 /graphene photocatalyst was hitherto reported for photocatalytic H_2 generation. It was reported that rGO could trap electrons from UV-irradiated TiO_2 via a percolation mechanism and transport the trapped electrons to reduce silver ions into silver nanoparticles. [21, 22] Transient photo voltage measurements also showed that the photovoltaic response of TiO_2 /graphene composite was positive, and the mean lifetime of electron-hole pairs was prolonged from $\sim 10^{-7}$ to $\sim 10^{-5}$ s in comparison with that of TiO_2. [23]. These findings directly proved that the photo induced electrons could transfer from TiO_2 to rGO to prevent their combination with the holes. Thus, graphene as an electron acceptor/transporter can promote the separation of the photogenerated electron-hole pairs in TiO_2 semiconductors, transport the photogenerated electrons to reactive sites efficiently, and finally improve the photocatalytic H_2 production. [24]

c. Graphene as a Co-catalyst

The co-catalyst is typically a noble metal or metal oxide or a combination of them, loaded on the surface of photocatalyst to enhance the charge separation, produce reactive sites, and Reduce the activation energy for gas evolution. Usually, noble metals possess higher work function than those of semiconductors, so deposition of noble metal nanoparticles onto the the surface of a semiconductor always makes electrons transfer from the CB of the exciting semiconductor to metal and results in the formation of a Schottkey barrier, which can efficiently

suppress the recombination of electrons and holes. Furthermore, most metals have much lower over potentials for H_2O reduction, indicating that they can provide plenty of reaction sites for absorbed protons. Therefore, noble metal co- catalysts have been widely applied for the enhancement of PEC/photocatalytic activities. However, noble metals are both costly and scarce. Thus much attention has been focused on seeking novel low-cost co- catalysts recently. Graphene with a high work function has been widely accepted to behave like metals, and the reduction potential of graphene/graphene is reported to be 0.08 eV, which is more negative than that of H^+ /H $_2$. [30]. Therefore, graphene is also a promising candidate for a cost-effective co- catalyst to replace noble metals.

d. Graphene as a Photocatalyst

Theoretical and experimental work [25,26] has demonstrated that the CB minimum of rGO, which is mainly formed by the anti-bonding π^* orbital, has a higher energy level (-0.52 eV vs NHE, pH $= 0$) than that needed for the H_2 generation, while the VB maximum of rGO is mainly composed of O 2p orbital that varies with the reduction degree .The band gap of rGO decreases with increasing reduction degree, suggesting that rGO with a suitable bandgap for water splitting might be obtained by tuning its reduction level. [8, 9] Yeh et al. [11] proved the photocatalytic H_2 evolution activity of rGO for the first time using the rGO sample with the bandgap of $2.4 - 4.3$ eV.

e. Graphene as a Photosensitizer

Graphene has been widely considered to accept electrons from photo excited semiconductors, as discussed above. However, the transfer of photo excited electrons from graphene to semiconductor has also been observed according to several experimental and theoretical researches. Very recently, a visible-light-response ZnS/rGO photo- catalysts were reported, and rGO in the nanocomposites was proved to act as an organic dye-like macromolecular "photosensitizer" instead of an electron reservoir for ZnS. [22] Similarly, other graphene-based wide bandgap semiconductors, such as TiO_2 /rGO and $ZnWO_4$ /rGO, also exhibited excellent photocatalytic activity in dye degradation under visible light irradiation owing to the photosensitization of graphene. [7] In these work, the photosensitizer role of graphene was explained as follows: the electrons on the HUMO of graphene were firstly excited to the LUMO of graphene under visible light irradiation, then the photo induced electrons in graphene were injected to the CB of semi- conductor followed by taking part in the reduction reaction on the surface of semiconductor, thus producing visible light activity.

2.4 Research Gaps

After reviewing the recent research papers, I find there is some scope to enhance the Hydrogen production rate that has not yet been explored or remains unexplored.

    I.   **Use of visible light active water adsorbent encapsulated photocatalyst having high water retention capacity for enhanced hydrogen production rate**

   II.   **Performance of Hydrogen generation by photocatalytic water splitting in batch as well as continuous mode using photocatalyst of high water retention capacity**

2.5. Objectives

    I.   Synthesis of water adsorbent alginate encapsulated visible light active **CdS-alginate** and **rGO-CdS-alginate** photocatalyst systems.

   II.   Characterization of synthesized photocatalyst.

  III.   Performance analysis of synthesized photocatalyst for enhanced hydrogen generation

  IV.   Calculation of photocatalytic activity and apparent quantum efficiency of above-mentioned photocatalytic systems.

<p align="center">********************</p>

Chapter-III

Experimental work and research methodology

3.1. Synthesis of Cadmium sulfide (CdS) by hydrothermal method:

Material required

Cadmium acetate Dihydrate ($\geq 98\%$), Thio-urea ($\geq 99\%$) and Sodium tungstate dihydrate ($\geq 99\%$) were purchased from Sigma-Aldrich. Ethanol ($\geq 99.9\%$; AR) was purchased from Jiangsu Huaxi international Trade Company limited. Sodium hydroxide pellets ($\geq 97\%$) was purchased from Merck Life Science Private Limited. Distilled water was purchased from a local supplier for making the solution. All reagents were used as received without further purification.

5.56 g of cadmium acetate was dispersed into 50 ml of DI water by stirring vigorously for 1 hour to obtain a 0.5 M cadmium acetate solution. Then 3.806 g of Thiourea was mixed into 50 ml of DI water and stirred for 1 hour. In the next step, these two solutions were mixed in a beaker, and the resulting solution underwent stirring at 80°c for 10 hours. Finally, we got CdS solution. The colour change was the indication of the formation of CdS solution. A yellow colour solution of CdS was formed. [17]
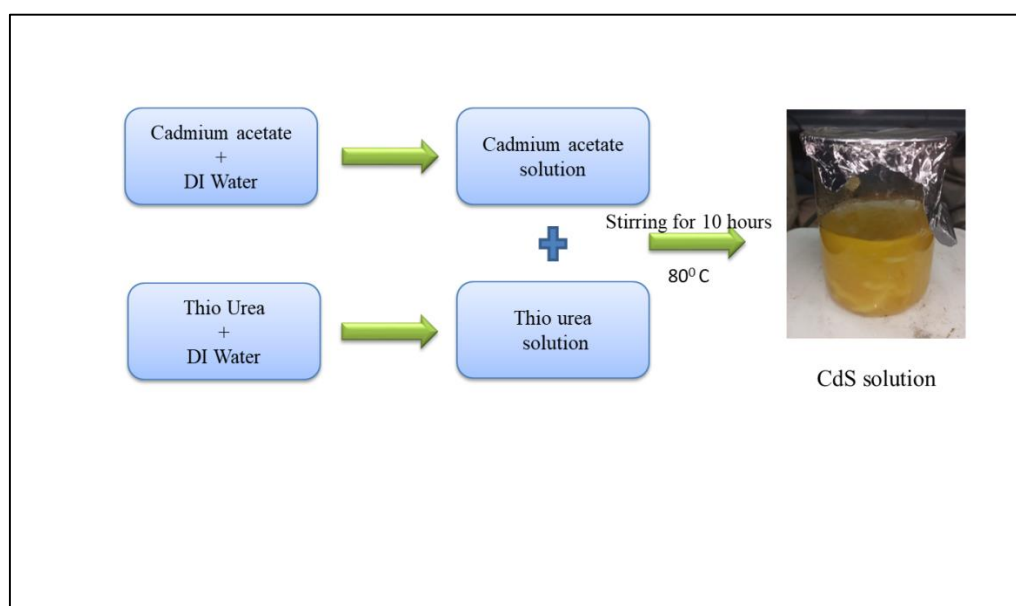

Fig. 3.1 Scheme of CdS photocatalyst

3.2. Synthesis of Graphene oxides (GO) by Improved Hummer's method

Materials required

1. Graphite flakes

2. Sulfuric acid (H_2SO_4)

3. Ortho-phosphoric acid (H$_3$PO$_4$)

4. Potassium permanganate (KMnO$_4$)

5. Hydrogen peroxide (H$_2$O$_2$)

6. Hydro-chloric acid (HCl)

7. Ethanol (C$_2$H$_5$OH)

8. Water (H$_2$O)

Graphene oxide (GO) was produced using modified hummers method from pure graphite powder. In this method, 27 ml of sulfuric acid (H$_2$SO$_4$) and 3 ml of phosphoric acid (H$_3$PO$_4$) (volume ratio 9:1) were mixed and stirred for several minutes. Then 0.225 g of graphite powder was added into mixing solution under stirring condition. 1.32 g of potassium permanganate (KMnO4) was then added slowly into the solution. This mixture was stirred for 6 hours until the solution became dark green. To eliminate excess of KMnO4, 0.675 ml of hydrogen peroxide was dropped slowly and stirred for 10 minutes. The exothermic reaction occurred and let it to cool down. 10 ml of hydrochloric acid (HCl) and 30ml of deionized water (DIW) was added and centrifuged using Eppendorf Centrifuge 5430R at 5000 rpm for 7 minutes. Then, the supernatant was decanted away and the residuals was then rewashed again with HCl and DI Water for 3 times. The washed GO solution was dried using oven at 90 °C for 24 hours to produce the powder of GO. [18]
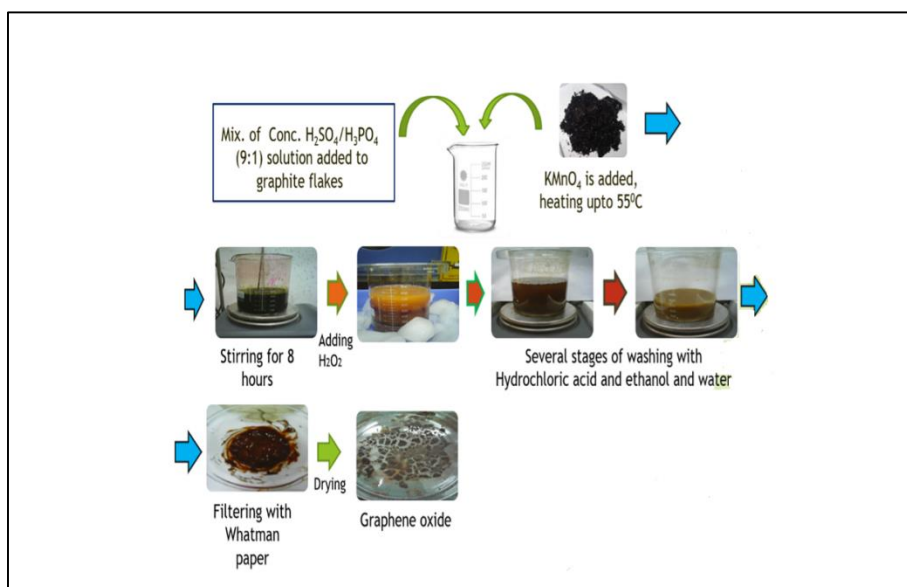

Fig. 3.2 Schematic of Synthesis of Graphene oxide (GO)

3.3 Synthesis of rGO-CdS nanocomposites:

Graphene oxide was synthesized from natural graphite flakes by the modified Hummer method. 0.1 g. of graphene oxide powder was ultrasonically dispersed in 50 ml of DI water for 1 hour in order to obtain the well-dispersed graphene oxide Nano sheets.

Subsequently, previously prepared CdS solution was added into the graphene oxide suspension under magnetic stirring at 80°c until a homogeneous mixture was formed. The final mixture was poured into a set of Teflon hydrothermal containers and then hydrothermally treated at 200°c for 18 hours in a muffle furnace. After cooled to room temperature, the sample was washed and centrifuged repeatedly with distilled water and ethanol, respectively. Then it was dried under a vacuum chamber at 70°c. Finally, the powder sample was obtained.
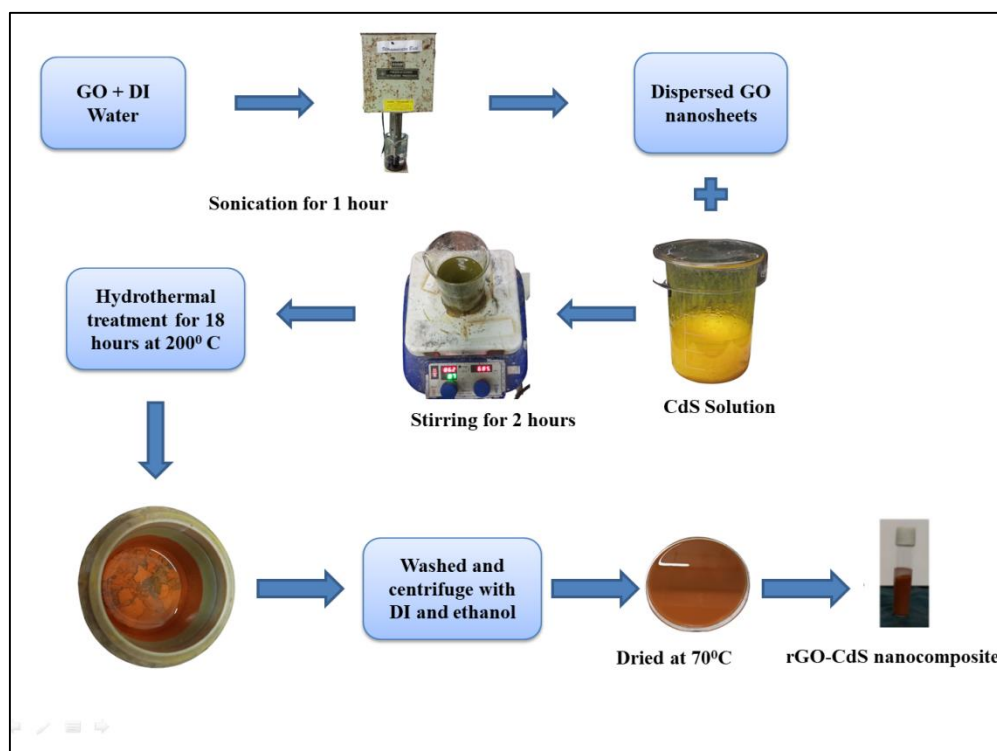
Fig. 3.3 Schematic of rGO-CdS nanocomposites synthesis

3.4 Preparation of rGO-CdS-Alginate encapsulated Photocatalyst

Materials required:

1. Sodium Alginate

2. rGO-CdS-photocatalyst in the form of powder

3. Calcium chloride

4. DI water

Synthesis procedure rGO-CdS-Alginate

At first, 1 g. of sodium alginate powder was mixed with 50 ml of deionized water in a beaker and stirred for 3 hours at 70^0C. Then 0.5 g. of previously synthesized rGO-CdS powder was mixed with 50 ml of water in another beaker and stirred for 2 hours at 70^0c. Alongside, 5 wt % $CaCl_2$ solution was prepared and placed in a petridish. Now the catalyst solution was mixed with sodium alginate solution and the resulting mixture was stirred for 20 hours at 80^0C. Now the resulting solution was placed in the $cacl_2$ contained petridish in the form of beads with the help of a syringe. After 24 hours the beads were washed by distilled water and contained in a bottle for further use.
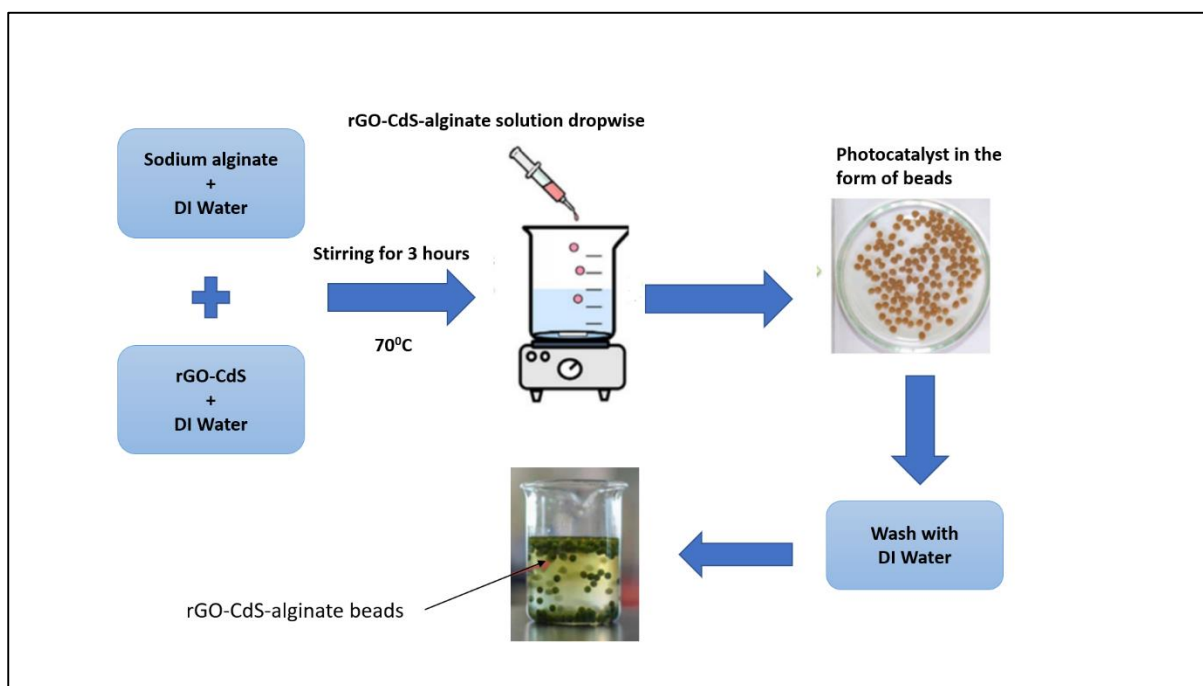

Fig. 3.4 Schematic of rGO-CdS- alginate Synthesis

3.5 Characterization of photocatalyst

- **UV-VIS Spectroscopy: Band gap**

A linear relationship between absorbance, the concentration of absorbers (or absorbing species) in the solution, and the route length is established by the Beer-Lambert law. As a result, for a fixed path length, UV-Vis spectroscopy can be used to determine the concentration of the absorbing species. This method is incredibly straightforward, adaptable, quick, precise, and economical. The UV-Vis-NIR Spectrophotometer is a tool used for ultraviolet-visible (or UV-Vis) spectroscopy. Utilizing radiative energy associated with the far and near ultraviolet (UV), visible (Vis) parts of the electromagnetic spectrum, this can be used to investigate liquids, gases, and solids. As a result, the following preset wavelengths have been established for these regions: UV: 300–400 nm; Vis: 400–765 nm.

Principle:

The wavelength of the light that reaches the detector after travelling through an object in a light beam is measured. Important details regarding the chemical structure and amount of molecules are revealed by the measured wavelength (present in intensity of the measured signal). As a result, information that is both quantitative and qualitative can be acquired. Information can be gathered through the transmittance, absorbance, or reflectance of photons with a wavelength between 160 and 3500 nm. The promotion of electrons to excited states or the anti-bonding orbitals results from the absorption of incident energy. Photon energy must match the energy required by an electron to be promoted to the next higher energy state in order for this transfer to take place. The fundamental idea behind absorption spectroscopy is this technique. There could be three different kinds of ground state orbitals at play: 1. Molecular (bonding) orbital 3. n (non-bonding) atomic orbital.

The sample absorbs some of the incident wave energy when focussed light with a certain wavelength and energy is directed at it. A photodetector monitors the energy of light that is transmitted from the sample and records the sample's absorbance. The light absorbed or transmitted by the sample is plotted against its wavelength to create the absorption or transmission spectrum. The Lambert-Beer rule, also known as the Bouguer-Beer law, is a fundamental tenet of quantitative analysis that states that a solution's absorbance scales directly with the concentration of analytes. The absorbance for a specific wavelength (unit less) A is the molar absorptivity of the absorbing species (M^{-1} cm^{-1}), B is the sample holder's route length (typically 1 cm), and C is the solution concentration (M). A = a. b. c. The UV-visible and near-infrared (NIR) spectrometer can measure absorbance or transmittance in this range. The following describes the relationship between incident light of intensity "I_o" and transmitted light of intensity "I." I/I_o provides transmittance (T), while $(I/I_o)*100$ provides transmission rate (T %). The formula for absorbance (abs), which is the opposite of transmittance, is

$$A = kcl = \log (I_0/I) \qquad\qquad 1\text{-}10$$

Here, the proportionality constant is denoted by k. While absorbance exhibits proportionality with sample concentration (Beer's law) and optical path (Bouguer's law), transmittance is independent of sample concentration. Additionally, k is referred to as a molar absorption coefficient and denoted as " when the optical path is 1 cm and the concentration of the targeted material is 1mol/l. The material's molar absorption coefficient is typical under certain circumstances. According to the Bouguer-Beer rule, there is no stray produced, scattered, or reflected light.
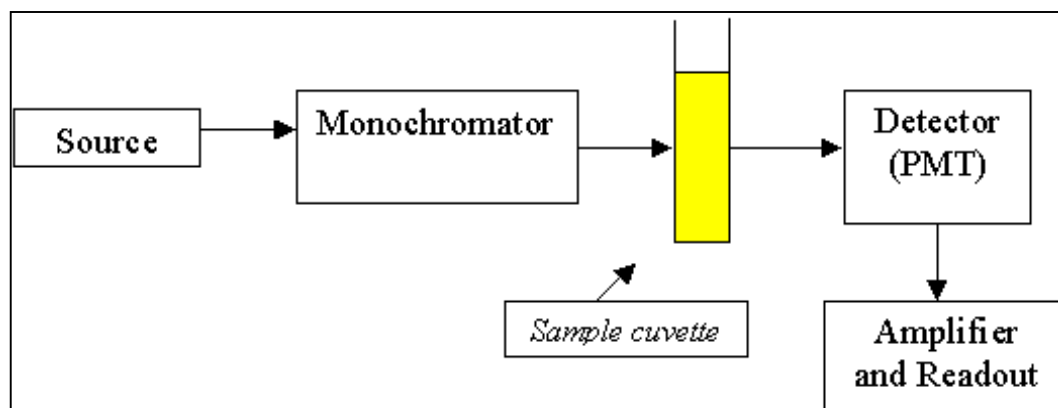
Fig. 3.5 Instrumental diagram of uv-vis spectrometer

Tauc relation: $(\alpha h\upsilon)^2 = A (h\upsilon - E_g)$ 1-12

α= absorbance

h= plank constant
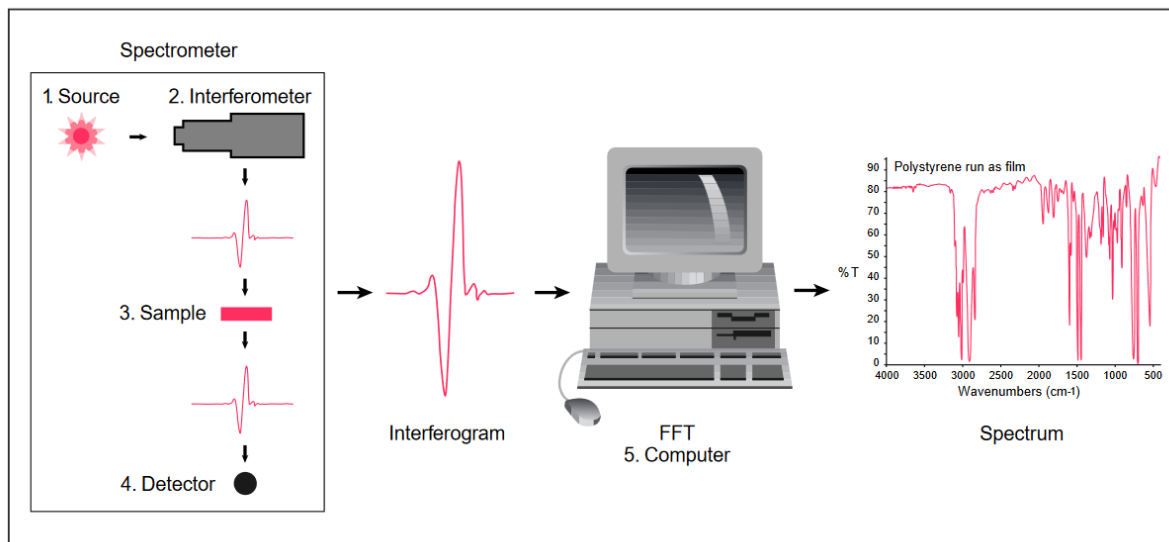
υ= frequency

E$_g$= band gap energy

Fig.3.6 Principle of UV-VIS spectroscopy

X-RAY diffraction (XRD)

X-ray diffraction (**XRD**) is the experimental science determining the atomic and molecular structure of a crystal, in which the crystalline structure causes a beam of incident X-rays to diffract into many specific directions. By measuring the angles and intensities of these diffracted beams, a crystallographer can produce a three-dimensional picture of the density of electrons within the crystal. From this electron density, the mean positions of the atoms in the crystal can be determined, as well as their chemical bonds, their crystallographic disorder, and various other information. [29]

Principle of XRD

XRD is based on constructive interference of monochromatic x-rays and a crystalline sample. These x-rays are generated from a cathode ray tube, filtered to produce monochromatic radiation directed towards the sample. The interaction of incident rays with the sample produces constructive interference when condition satisfy **Bragg's law**.
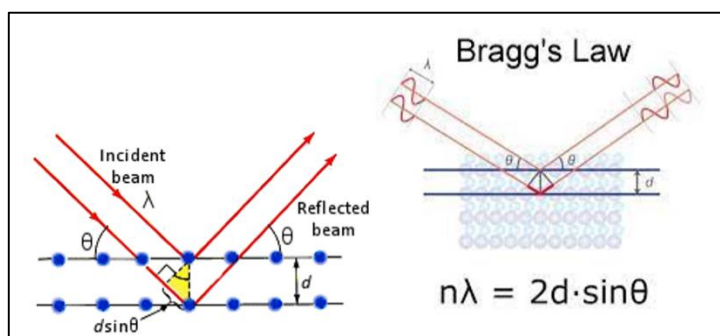
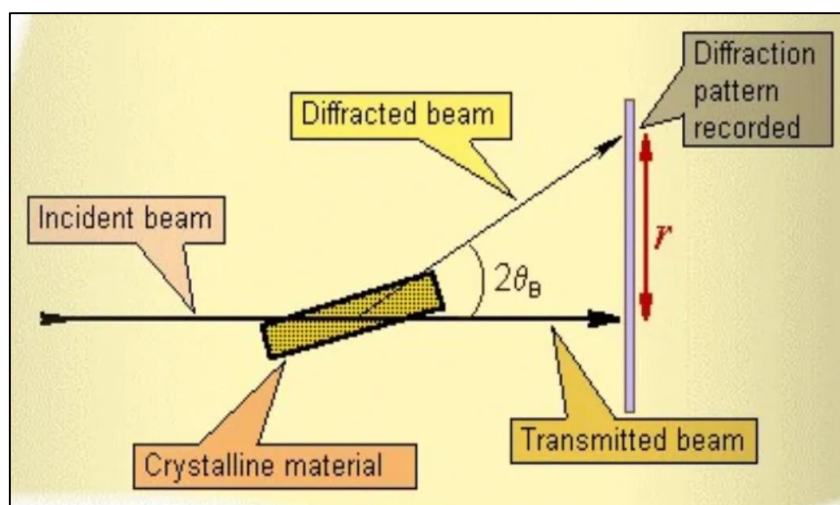**Fig. 3.7 Visualisation of Bragg's law**
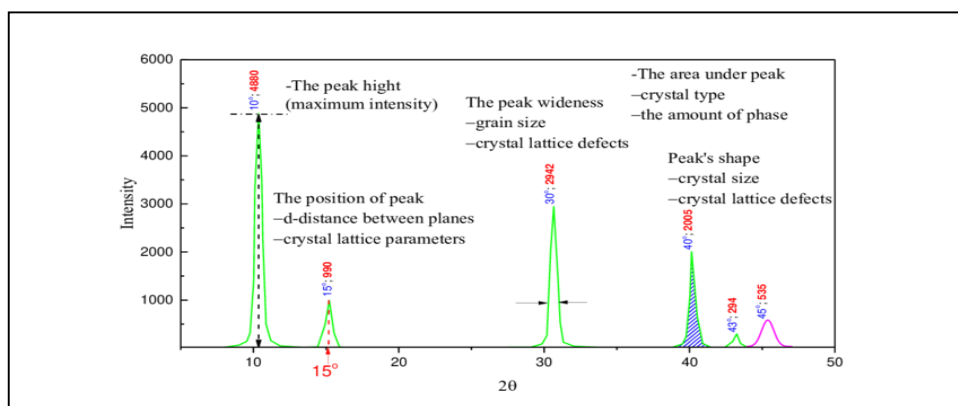

Fig 3.8 Principle of XRD

Fig. 3.9 Different peaks in XRD

The **Scherrer equation** is used in the determination of size of crystals in the form of powder.

The Scherrer equation can be written as:

$$D = K\lambda/\beta Cos\theta \qquad\qquad 1\text{-}13$$

D = Mean Crystallites size (nm)

K =0.9 (Scherrer constant)

λ =0.15406 nm (wavelength)

β = FWHM (radians)

θ = peak positions (radians)

3.6 Design of photo reactor

A laboratory-scale photo-reactor (volume of the reaction vessel: 50 ml.) setup was used for the performance analysis of different photocatalysts. This reactor was operated in batch mode of operation. There were several components of the reactor.

I. Solar simulator as source of light

II. Reaction Vessel

III. Gas outlet

IV. Water displacement unit
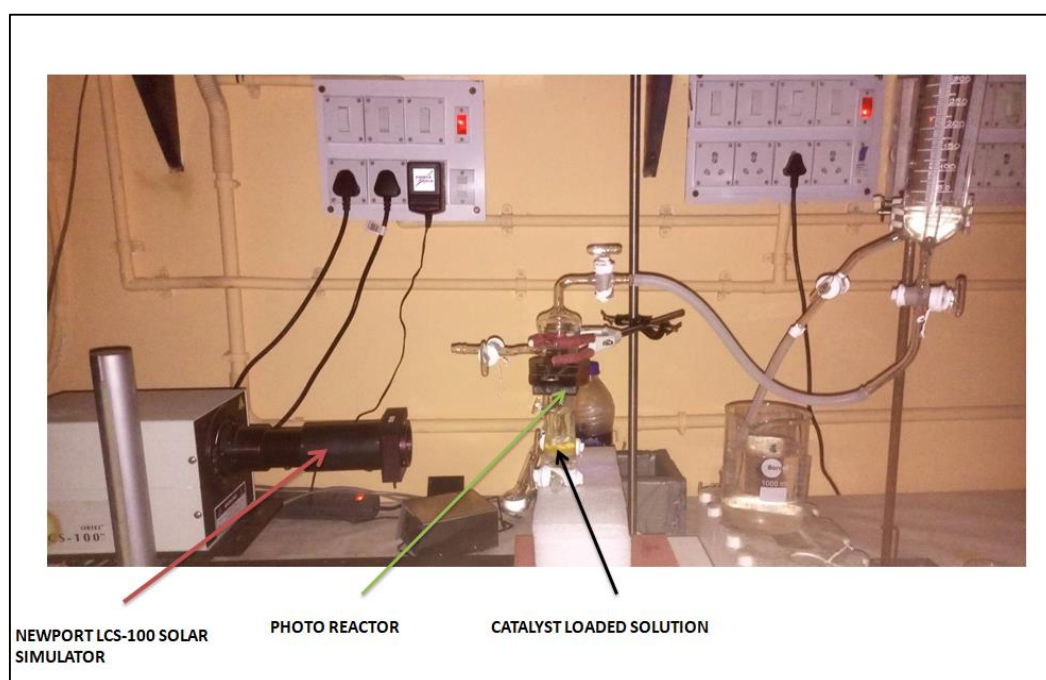
V. Control Valve

Schematic of Reactor Set-up

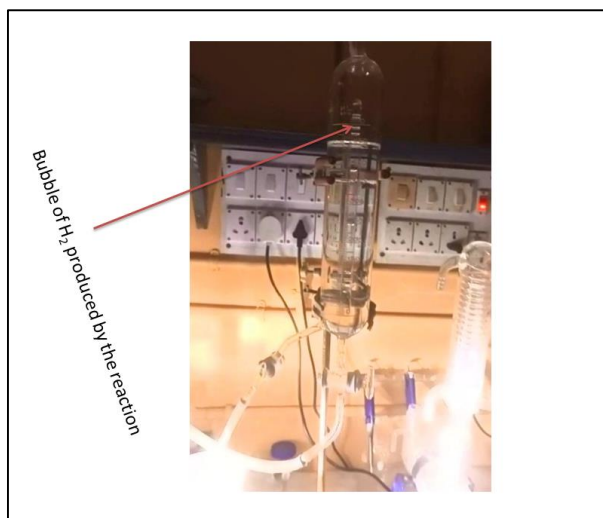**Fig. 3.10 Experimental set up**

Fig. 3.11 Hydrogen generation in the form of bubble

Solar Simulator

A solar simulator is a device whose light source offers similar intensity and spectral composition to natural sunlight. Solar simulators (also called "sunlight simulators") are scientific equipment used to replicate sunlight in controlled laboratory environment. In our work, we have used Oriel LCS-100TM small area Sol.1A series solar simulator which is integrated, compact and easy to operate.

Fig 3.12 Newport LCS-100 Solar simulator

Band pass filter

Optical band pass filters are optical filters that pass one or more specified wavelength band(s) while blocking others. They basically chop off the required spectrum of light. Band pass filter is used to calculate apparent quantum yield of different photocatalytic systems.

Principle of working of solar simulator

a. A Xenon short arc lamp is energized by a power supply and is located inside an elliptical reflector which collects a high percentage of its output. The lamp's output is refocused near an optical homogenizer assembly.

b. The homogenizer, working together with the ellipse and the condenser lens, creates uniform illumination. Mirrors are used to fold the optical path as needed for the work.

c. Filter is located just before the homogenizer assembly to assure reproducible spectral shaping across the whole work plane.

d. The optical shutter is located after the spectral Filter and the homogenizer so that those optical elements and their mounts can come to thermal equilibrium after the
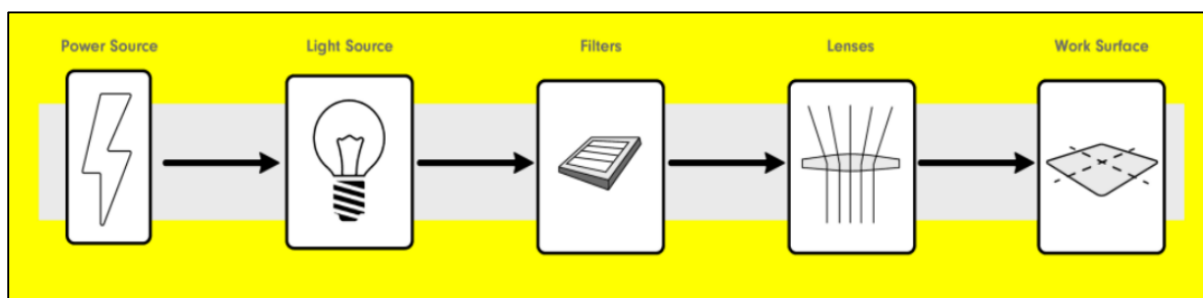
initial system warm-up and deliver stable performance.

Fig 3.13 Principle of working of solar simulator

3.7 Performance Study and analysis:

3.7.1 performance Study

For a particular experimental study, 25 ml of deionized water was used and the pH and the dissolved solid of the water were checked using a portable pH/EC/TDS checker (Hanna Instruments, USA; HI991300P) which were 6.53 and 0.009 ppm, respectively. A Solar simulator (94011A, Manual shutter, Newport Oriel LCS-100) was utilized to simulate and the intensity was adjusted to 100 mW.cm^{-2}. The Solar Simulator includes an AM 1.5G air mass filter which provides Class A spectral performance based on current applicable standards at 1 sun irradiance output. Alginate encapsulated photocatalyst soaked

in water (without solar irradiation) for 12 hrs was used for photocatalysis. Evolved hydrogen was collected and measured by displacement of water column.

3.7.2 Performance Analysis

To quantify the role of photocatalyst the following performance parameters were evaluated:

Activity of photocatalyst

Moles of hydrogen generated is calculated from the volume of water displaced in the system. The volume in ml is converted to mmol. Photocatalytic activity defined as moles of Hydrogen generated/g photocatalyst .h) denotes the effectiveness of the catalyst. It is the amount of hydrogen generated per unit mass of photo-catalyst (excluding the mass water adsorbent alginate) used per unit time.

Apparent Quantum Yield (AQY)

It is defined as the ratio of the number of emitted photons divided by the number of absorbed photons. To obtain high solar energy conversion efficiency, the quantum efficiency of photocatalytic reaction must be increased over a wide range of wavelengths. If a photon (E_{photon}) of wavelength of λ_{inc} (nm) is incident during a photocatalytic water splitting reaction, the energy of this one photon calculated using the equation:

$$E_{photon} = \frac{hc}{\lambda_{inc}} \qquad \qquad 1\text{-}14$$

where h (J·s) is Planck's constant,

c (m·s^{-1}) is the speed of light
λ_{inc} (m) is the wavelength of the monochromatic light that is incident.
And the total energy of the incident monochromatic light (E_{total}) is calculated using the following equation:
$$E_{total} = P\, s\, t \qquad \qquad 1\text{-}15$$
P (W·m^{-2}) is the power density of that incident monochromatic light,
S (m^2) is area that is being irradiated
t (s) is the duration of the exposure of the incident light
The total number of incident photons can be determined from the given equation:
$$\text{Number of incident photons} = \frac{E_{total}}{E_{photon}} = \frac{P\, s\lambda_{inc}\, t}{hc} \qquad \qquad 1\text{-}16$$
This can be seen from the equation

$$\text{A.Q.Y } (\%) = \frac{2 n_{H2,t}\, N_A\, hc}{P\, s\lambda_{inc}\, t} \times 100 \qquad \qquad 1\text{-}17$$

Where $nH_{2,t}$ (mol) is number of molecules of Hydrogen evolved over the duration t of the incident light

N_A (mol^{-1}) is Avogadro's constant [25].

****

Chapter-IV

Result and

Discussion

4. Result & Discussion

Experimental result:

4.1 UV-Vis Study

The optical absorption properties of CdS, rGO-CdS and rGO-CdS-alginate were extensively investigated by Ultraviolet-visible spectroscopy (Figure 4.1). The optical band gap energies were calculated by Tauc plot method. The pristine CdS showed a strong absorption at around 550 nm which attributed to the narrow band gap. Sodium alginate gave weak absorption spectra at 210 nm and showed almost no visible light absorption. After the addition of CdS, the CdS-alginate shows an intensive light absorption intensity and extended photo responding range. The Sodium alginate exhibited similar absorption edge as compared with pristine CdS. From UV spectra it can be found that the peaks were obtained at 407 nm, 353 nm and 390 nm for pristine CdS, CdS- Alginate and rGO-CdS-Alginate, respectively. /
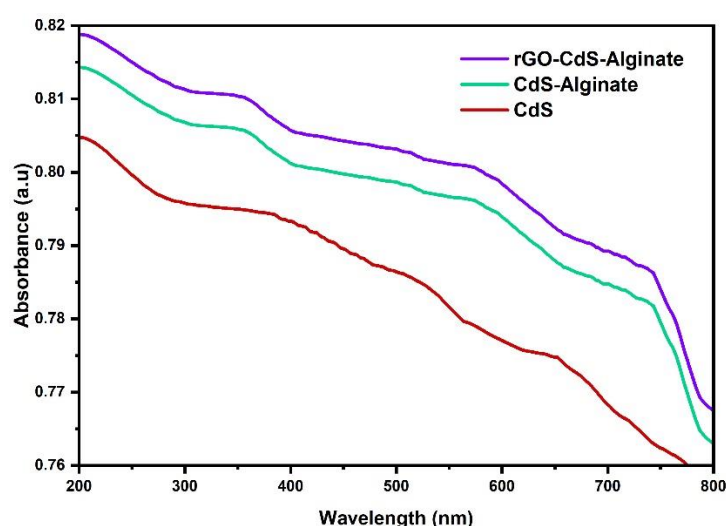

Fig. 4.1 UV-VIS spectroscopy of different synthesized catalyst

Tauc Plot

Meanwhile, the absorption edges displayed a slight red-shift with the increase of CdS loading. This indicated that the sodium alginate can harvest the visible light to generate photoelectrons and holes efficiently. The calculated band gaps derived from Tauc plot method were 2.4 eV for CdS, 3 eV for CdS-Sodium Alginate and 2.33 eV for rGO-CdS-alginate, as seen in Fig (4.2). These results are in agreement with previous reports. It is found that after addition of CdS in the sodium alginate the E_g value increased but after the addition of rGO the E_g value decreased than the pristine CdS. Therefore, it can be predicted that with the loading of graphene, the band gap of the CdS-alginate composite

gradually decreases, which might be effective in minimizing the rate of recombination of photogenerated electron-holes.
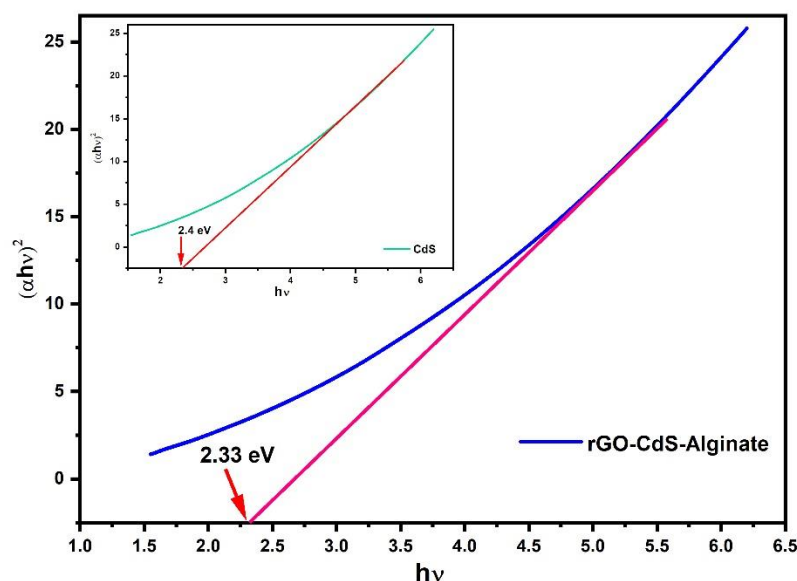

Fig. 4.2 Tauc Plot

4.2 XRD analysis

Figure (4.3) delineates the XRD analysis of the CdS, CdS-alginate and rGO-CdS–alginate micro sphere photo catalyst. The peak splitting observed at 24.82, 26.52, 28.20, 36.62, 43.72 and 52.85 of 2θ corresponds to the structure of CdS (JCPDS card no. 14-0133) match well with hexagonal wurtzite phase of CdS and can be indexed respectively to the (1 0 0), (0 0 2), (1 0 1), (1 0 2), (1 1 0), (2 0 1) crystal planes. There is a weak and broad peak centred at 21.6 that belongs to sodium alginate. The crystalline peaks of CdS-alginate were similar to CdS indicates that the crystal structure is maintained in organic hydrogel framework. With the increase in CdS loading amplified (111) peak demonstrated that the crystallinity increased. However, when the mass ratio of alginate to CdS was RCA 1:2, the peak intensity decreased compared to RCA 1:5. This is probably due to the excess loading of rGO-CdS leading to aggregation. The right shift of the (111) crystal plane is ascribed to the interfacial interactions between CdS and Sodium alginate chains.
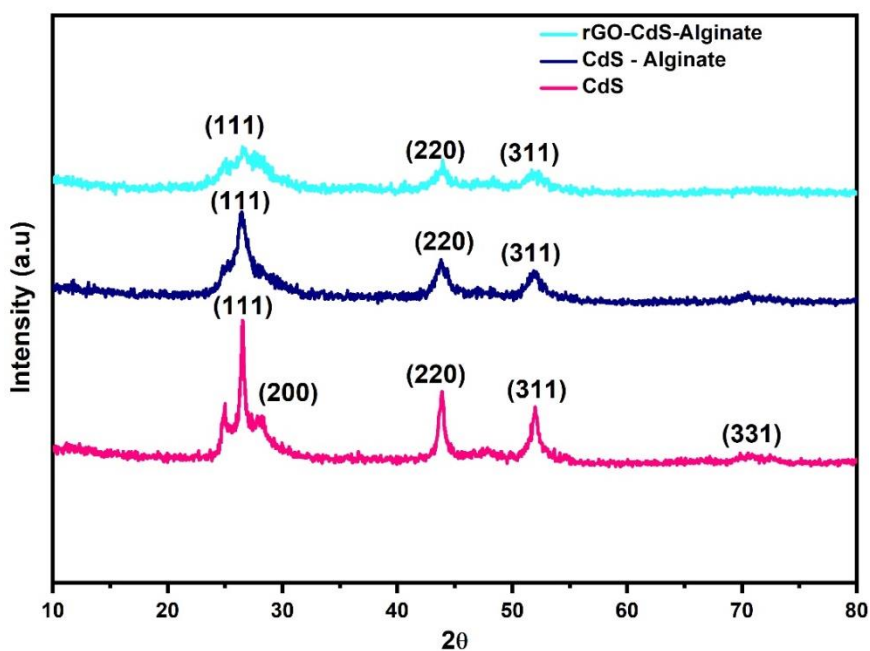
Fig. 4.3 The XRD patterns CdS, CdS-alginate and rGO-CdS-alginate

4.3 Performance study of different photocatalyst:

In this chapter, the synthesized photocatalysts are studied and analysed Moles of Hydrogen generated

- ✓ Activity of the photocatalysts
- ✓ Apparent Quantum Yield of the process

1. **Generation of Hydrogen using synthesized CdS and rGO-CdS photocatalyst**
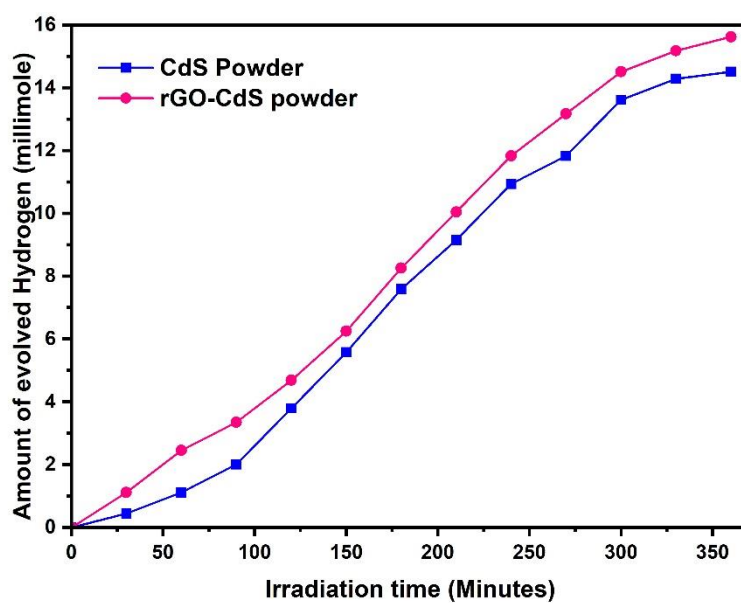
Fig. 4.4 Moles of hydrogen evolved vs. time plot of CdS an rGO-CdS

2. **Generation of Hydrogen using synthesized CdS-alginate photocatalyst**

Here the following table shows the moles of hydrogen generation with respect to time. With increasing time hydrogen generation increased using CdS- alginate. The following experiment is conducted using three condition.

➢ Full band of solar spectrum
➢ 420 nm of solar spectrum
➢ 350 nm of solar spectrum

Full band of Solar spectrum

Time(Min)	Moles of Hydrogen generated(mmol)
0	0
50	23.43
100	49.77
150	71.87
200	83.92
250	101.56
300	117.19

Table 4.1 Moles of hydrogen generation of CdS-alginate with time

Comparative analysis of CdS-sodium alginate:

So, we can see that the moles of Hydrogen generated are greater in case of full band of solar spectrum and is slowly decreasing when we move to 420 nm and 350 nm consequently.

Wavelength	Moles of Hydrogen generated
Full Band	139.06
420 nm	98.56
350 nm	81.20

Table 4.2 Moles of hydrogen generation of CdS-alginate at different wavelength of solar spectrum
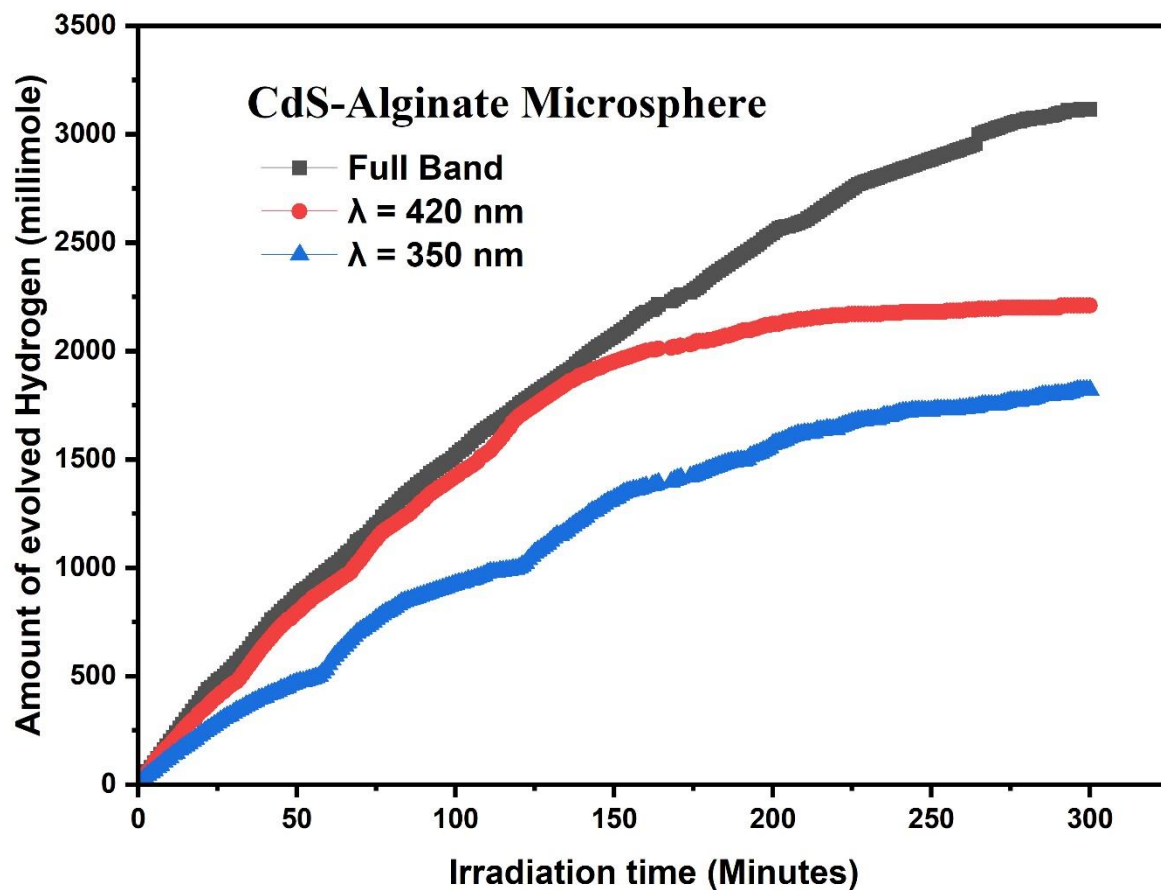

Fig 4.5 Moles of Hydrogen generated vs time plot using different band pass filter with CdS-alginate.

3. Performance analysis of rGO-CdS- alginate

Full band of solar spectrum

Time (Min)	Moles of Hydrogen generated (mmol)
0	0
50	39.73
100	72.99
150	93.30
200	106.03
250	115.40
300	126.34
350	135.04

Table 4.3 Moles of hydrogen generation of rGO-CdS-alginate with time

Comparative analysis of rGO-CdS- alginate:

So it is clearly visible that the inclusion of reduced graphene oxide can enhanced the hydrogen generation by a great margin. And the hydrogen generation is at its peak when we use full band of solar spectrum.

Wavelength	Moles of Hydrogen generated
Full Band	239.06
420 nm	98.88
350 nm	93.75

Table 4.4 Moles of hydrogen generation of rGO-CdS-alginate at different wavelength of solar spectrum
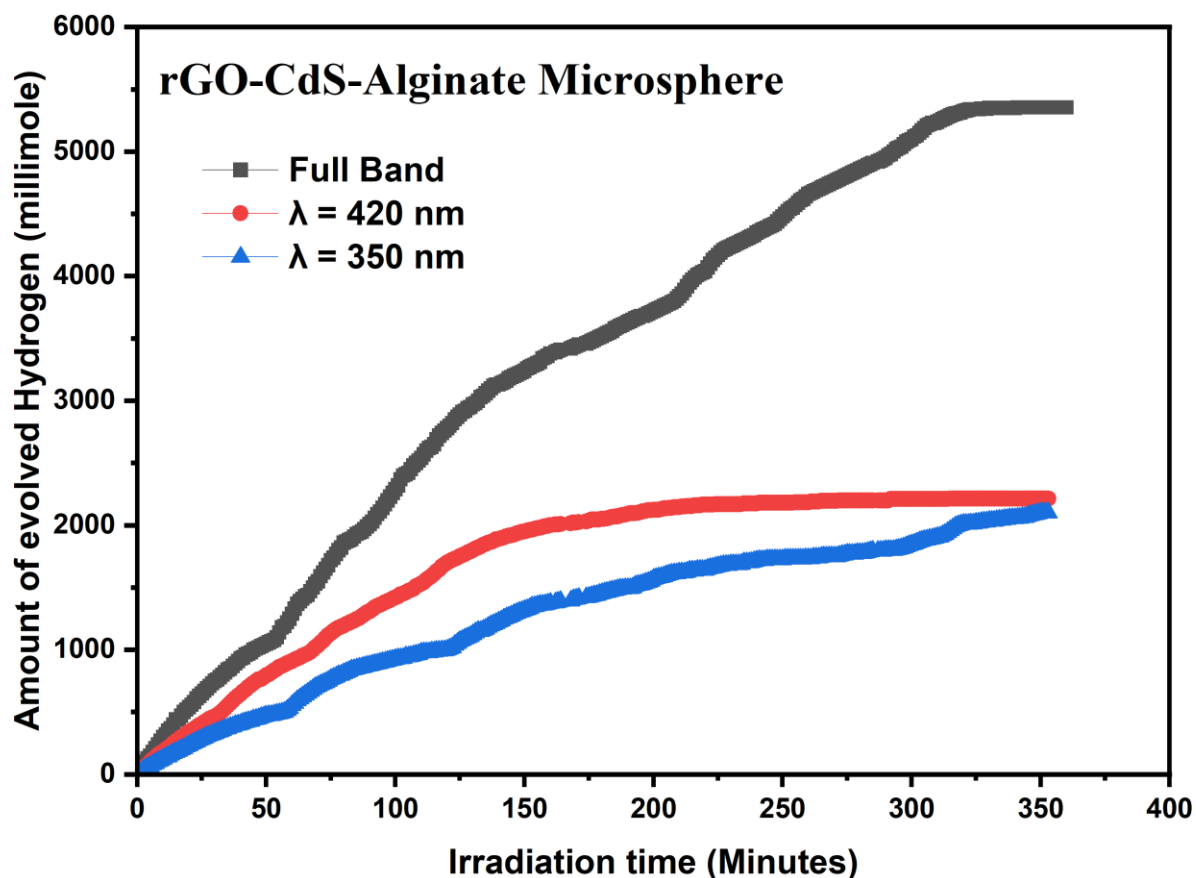
Fig. 4.6 Moles of Hydrogen generated vs time plot of rGO-CdS- alginate catalyst

4. Comparative performance analysis of different photocatalyst:

Catalyst name	Moles of Hydrogen generated(mmoles) in 6 hrs
CdS	14.50
rGO-CdS	16.62
CdS- alginate	139.06
rGO- CdS- alginate	239.06

Table 4.5 Comparative performance analysis of different photocatalyst

Photocatalytic activity of different photocatalyst:

Photocatalytic activity (moles of Hydrogen generated/g.h) of photo catalyst characterize the effectiveness of the catalyst.

Catalyst	Photocatalytic activity (mmoles/gm.hr)
CdS	4.88
rGO-CdS	5.20
CdS-Alginate	55.62
rGO-CdS-Alginate	79.68

Table 4.6 activity of synthesized photocatalyst

So the photocatalytic activity is maximum for rGO-CdS- alginate photocatalytic system at the full band of the solar spectrum.
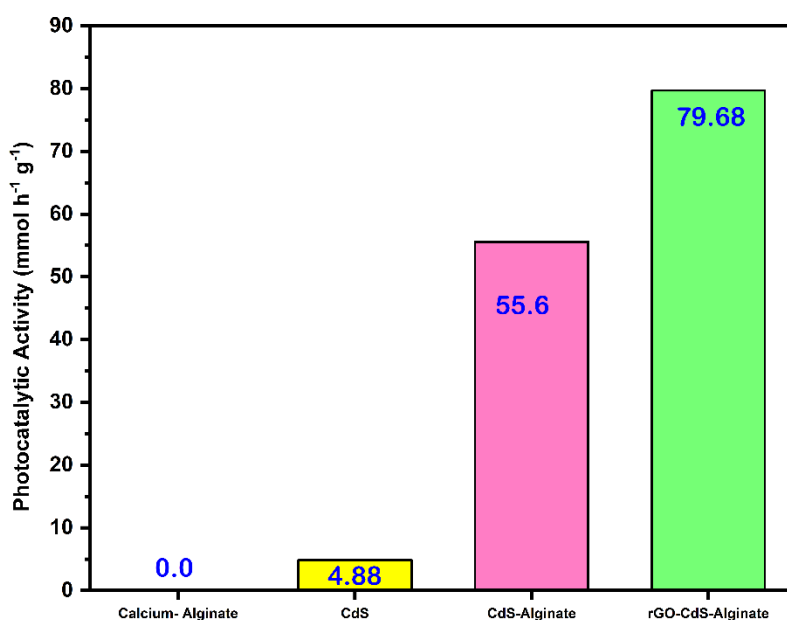

Fig. 4.7 Activity of different photocatalyst

Apparent Quantum Yield (AQY) study of different photocatalyst:

It is defined as the ratio of the number of emitted photons divided by the number of absorbed photons. To obtain high solar energy conversion efficiency, the quantum efficiency of photocatalytic reaction must be increased over a wide range of wavelengths.

$$Q.Y. (\%) = \frac{\text{Number of reacted electrons}}{\text{Number of incident photons}} \times 100 \qquad \text{1-18}$$

Apparent Quantum Yield analysis of CdS- alginate photocatalyst at different band pass filter:

Catalyst name	Band Pass filter	(AQY)%
rGO-CdS- alginate	420 nm	18.4

Table 4.7 Apparent quantum yield of synthesized photocatalyst

****

Chapter-V

Conclusion

5. Concluding Remarks

As a new type of carbon nanomaterial, graphene has been widely used in the creation of H_2 via light-driven water splitting. It not only demonstrates the ability to separate photogenerated electron-hole pairs, supersede noble metals, increase photo stability, and expand light absorption, but it also demonstrates the capability for photocatalytic H_2 evolution. Nonetheless, research on graphene-based materials for H_2 generation from light-driven water splitting is still in its early stages, and there are numerous hurdles that must be overcome in order to significantly improve photocatalytic performance or maybe lead to breakthrough. Some of the findings are listed as follows:

- A highly active, reduced Graphene oxide based water adsorbent (Sodium alginate) mediated visible light active hybrid photocatalyst named as **rGO-CdS-alginate** is proposed for enhanced hydrogen production by photocatalytic water splitting.

- The study of comparative analysis of photocatalytic activity is examined using four different synthesized photocatalyst CdS, rGO-CdS, CdS-alginate, and rGO-CdS-alginate. Based on the comparative activity analysis of different photocatalyst, it is concluded that the photocatalytic activity of **rGO-CdS- alginate** is the maximum and it is recorded as **79.68 mmol/g.hr** which is remarkably higher than that of pristine CdS (4.88 mmol/g.hr)

- In the next phase of the research work, efficiency of the hydrogen generation by the synthesized photocatalysts was also examined. From the experimental result it is found that the AQY of **rGO-CdS-alginate** at **420 nm** is 18.4 %.

- It may be inferred that use of alginate having plenty of OH- groups promotes the water adsorption into its confined porous structure and causes the chemisorption of water molecules on the surface of photocatalyst (CdS/ rGO-CdS).

- Encapsulation of Cadmium sulfide based photocatalyst by alginate hydrogel not only enhances the hydrogen generation performance remarkably but also helps in circumventing toxic and carcinogenic effects of CdS.

�֍�֍✻✻✻✻✻✻✻✻

Chapter-VI

References

6. References

[1] Ahmad H, Kamarudin SK, Minggu LJ, Kassim M. Hydrogen from **photocatalytic water splitting process:** Renew Sust Energy Rev 2015;43:599e610.

[2] Gupta NM**. Factors affecting the efficiency of a water splitting photocatalyst: a perspective.** Renew Sust Energy Rev 2016; 71:585e601.

[3] Dubey PK, Tripathi P, Tiwari RS, Sinha ASK, Srivastava ON. **Synthesis of reduced graphene oxide TiO_2 nanoparticle composite systems and its application in hydrogen production**. Int J Hydrogen Energy 2014; 39:16282e92.

[4] Tee SY, Win KY, Teo WS, Koh LD, Liu S, Teng CP, et al. **Recent progress in energy-driven water splitting**. Adv Sci 2017; 4:1600337.

[5] Acar C, Dincer I. **Impact assessment and efficiency evaluation of hydrogen production methods**. Int J Energy Res 2015; 39:1757e68.

[6] Zhu J, Zeach M. **Nanostructured materials for photocatalytic hydrogen production**. Colloid Interface Sci 2009; 14:260e9.

[7] Muradov N, Veziroglu T. **"Green" path from fossil-based to hydrogen economy: an overview of carbon-neutral technologies.** Int J Hydrogen Energy 2008; 33:6804e39.

[8] Fujishima A. **Electrochemical photolysis of water at a semiconductor electrode**. Nature 1972; 238:37e8.

[9] Pulido Melian E, Gonzalez Dı́az O, Ortega Mendez A, Lopez CR, Nereida Suarez M, Dona Rodrı guez JM, et al. **Efficient and affordable hydrogen production by water photo-splitting using TiO_2-based photocatalysts**. Int J Hydrogen Energy 2013; 38:2144e55.

[10] Lin Y, Jiang Z, Zhu C, Hu X, Zhu H, Zhang X, et al. **The optical absorption and hydrogen production by water splitting of (Si, Fe)-cooped anatase TiO_2 photocatalyst**. Int J Hydrogen Energy 2013; 38:5209e14.

[11] Ye S, Wang R, Wu M-Z, Yuan Y-P. **A review on g-C_3N_4 for photocatalytic water splitting and CO_2 reduction**. Appl Surf Sci 2015; 358:15e27.

[12] Li H, Tu W, Zhou Y, Zou Z. **Z-scheme photocatalytic systems for promoting photocatalytic performance: recent progress and future challenges**. Adv Sci 2016; 3:1500389.

[13] Boudjemaa A, Rebahi A, Terfassa B, Chebout R, Mokrani T, Bachari K, et al. **Fe$_2$O$_3$/carbon spheres for efficient photocatalytic hydrogen production from water and under visible light irradiation.** Sol Energy Mater Sol Cells 2015; 140:405e11.

[14] Ling C, Xue Q, Han Z, Zhang Z, Du Y, Liu Y, et al. **High hydrogen response of Pd/TiO$_2$/SiO$_2$/Si multilayers at room temperature**. Sens Actuators B 2014; 205:255e60.

[15] Bahruji H, Bowker M, Davies PR, Pedrono F. **New insights into the Mechanism of photocatalytic reforming on Pd/TiO$_2$.** ApplCatal B 2011; 107:205e9.

[16] Umer M, Tahir M, Azam MU, Jaffar MM. **Metals free MWCNTs-TiO$_2$-MMT heterojunction composite with MMT as a mediator for fast charges separation towards visible light driven photocatalytic hydrogen evolution**. Appl Surf Sci 2019; 463:747e57.

[17] Yingchun Yu, Youxian Ding, Shengli Zuo, and Jianjun Liu, **Photocatalytic Activity of Nanosized Cadmium Sulfides Synthesized by Complex Compound Thermolysis**, Int J Photoenergy. 2011 (2010) 1-5.

[18] Daniela C. Marcano et al, **Improved Synthesis of Graphene Oxide, ACS Nano 4 (2010) 4806-4814.**

[19] Majid Ahmadi, Reza Younesi and Maxime J-F Guinel. **Synthesis of Tungsten Oxide Nanoparticles using a Hydrothermal Method at Ambient Pressure.**

[20] Clarizia L, Spasiano D, Di Somma I, Marotta R, Andreozzi R, Dionysiou DD. **Copper modified-TiO$_2$ catalysts for hydrogen generation through photo reforming of organics. A shor review**. Int J Hydrogen Energy 2014; 39:16812e31.

[21] Dincer I, Acar C. **Review and evaluation of hydrogen production methods for better sustainability.** Int J Hydrogen Energy 2015; 40:11094e111.

[22] Kondarides DI, Daskalaki VM, Patsoura A, Verykios XE **Hydrogen production by photo-**

induced reforming of biomass components and derivatives at ambient conditions. Catal Lett 2007; 122:26e32.

[23] Tahir M, Amin NS. **Advances in visible light responsive titanium oxide-based photocatalysts for CO$_2$ conversion to hydrocarbon fuels**. Energy Convers Manage 2013; 76:194e214.

[24] Chouhan N, Ameta R, Meena RK, Mandawat N, Ghildiyal R. **Visible light harvesting Pt/CdS/Co-doped ZnO Nano rods molecular device for hydrogen generation**. Int J Hydrogen Energy 2016; 41:2298e306.

[25] Yao-Guang Yu, Gang Chen, Lin-Xing Hao, Yan-Song Zhou, Yu Wang, Jian Pei, Jing-Xue Sun and Zhong-Hui Han. **Doping La into the depletion layer of Cd0.6Zn0.4S photocatalyst for efficient H$_2$ evolution**

[26] Acar C, Dincer I, Zamfirescu C. **A review on selected heterogeneous photocatalysts for hydrogen production**. Int J Energy Res 2014; 38:1903e20.

[27] Xu Y, Xu R. Nickel**-based cocatalysts for photocatalytic hydrogen production**. Appl Surf Sci 2015; 351:779e93.

[28] Wen J, Xie J, Chen X, Li X. **A review on g-C$_3$N$_4$-based photocatalysts**. Appl Surf Sci 2017; 391:72e123.

[29] Pandian Bothi Raja, Kabilashen Readdyi Munusamy, Veeradasan Perumal, Mohamad Nasir, Mohamad Ibrahim, **Nano-Bioremediation : Fundamentals and Applications**, Micro and Nano Technologies, 2022(57-83).

[30] Etacheri V, Di Valentin C, Schneider J, Bahnemann D, Pillai SC. **Visible-light activation of TiO$_2$ photocatalysts advances in theory and experiments**. J Photochem Photobiol C 2015; 25:1e29.

[31] Wenjun Luo, Zaisan Yang, Zhaosheng Li, Jiyuan Zhang, Jianguo Liu, Zongyan Zhao, Zhiqiang Wang, Shicheng Yan, Tao Yu and Zhigang Zou , **Solar hydrogen generation from seawater with a modified BiVO$_4$ photoanode**, Energy Environ. Sci., 2011, 4, 4046, DOI: 10.1039/c1ee01812d.

[32] Guancai Xie , Kai Zhang , Beidou Guo , Qian Liu , Liang Fang , and Jian Ru Gong, **Graphene-Based Materials for Hydrogen Generation from Light-Driven Water Splitting**, Adv. Mater. 2013, DOI: 10.1002/adma.201301207

[33] Xiaobo Chen, Shaohua Shen, Liejin Guo, and Samuel S. Mao, **Semiconductor-based Photocatalytic Hydrogen Generation**, Chem. Rev. 2010, 110, 6503–6570, doi: 10.1021/cr1001645.

[34] Beyza Nur Kinsiz , Bilge Cos̡ kuner Filiz, Serpil Kılıç Deprenc , Aysel Kantürk Figen, **Nanocasting procedure for catalytic cobalt oxide bead preparation from calcium-alginate capsules: Activity in ammonia borane hydrolysis reaction,** Applied materials today 22 (2021) 100952, https://doi.org/10.1016/j.apmt.2021.100952

[35] Akihiko Kudo, Yugo Miseki, **Heterogeneous photocatalyst materials for water splitting**, Chem. Soc. Rev., 2009, 38, 253–278, DOI: 10.1039/b800489g

[36] J.C. Murillo-Sierra, A. Hernández-Ramírez , L. Hinojosa-Reyes, J.L. Guzmán-Mar, **A review on the development of visible light-responsive WO$_3$-based photocatalysts for environmental applications**, Chemical Engineering Journal Advances 5 (2021) 100070, Chemical Engineering Journal Advances 5 (2021) 100070, https://doi.org/10.1016/j.ceja.2020.100070

[37] Xiaoling Lang,, Saianand Gopalan, Wanlin Fu, Seeram Ramakrishna, **Photocatalytic Water Splitting Utilizing Electrospun Semiconductors for Solar Hydrogen Generation: Fabrication, Modification and Performance**, Bull. Chem. Soc. Jpn. 2021, 94, 8–20 | doi:10.1246/bcsj.20200175

[38] Nur Fajrina, Muhammad Tahir, **A critical review in strategies to improve photocatalytic water splitting towards hydrogen production**, jhydene.2018.10.200, https://doi.org/10.1016/j.ijhydene.2018.10.200

[39] Kok Yuen Koh, Zhihao Chen, Zhongrong Du, Sikal Benjamin Ngeow, J.Paul Chen, **A visible light-driven photocatalysis process by alginate beads coupled with in-situ cadmium sulfide prepared for decontamination in aqueous solutions with treatment of chromium as an example**, Chemical engineering journal advances. 2022.11, https://doi.org/10.1016/j.ceja.2022.100356.